Physics – Uspekhi **39** (8) 781 – 805 (1996)

REVIEWS OF TOPICAL PROBLEMS PACS number: **75.90.+w**

Lanthanum manganites and other giant-magnetoresistance magnetic conductors

E L Nagaev

Contents

Abstract. A review is given of crystallographic, magnetic and electric properties of lanthanum manganites and related materials with a giant magnetoresistance (GMR). An analysis of experimental data for partially substituted manganites shows that if the spontaneous magnetic moment is unsaturated, the material is being in a phase-separated ferro-antiferromagnetic state. One possible GMR mechanism consists in a change of such a state under the magnetic field. If the magnetic moment of these materials is saturated, they display a resistivity peak in the vicinity of the Curie point. It is caused by the interaction of the charge carriers with spatial fluctuations of the electric potential and local magnetization. Suppression of this peak by the magnetic field leads to a GMR in ferromagnetic conductors.

1. Introduction

Actual problems of the microelectronics make it highly desirable to construct devices with large isotropic negative magnetoresistance and functioning at room temperatures. In particular, they are required for magnetic recording and reading heads, for reliable storage of information, etc. In recent years the main line of activity in this direction was development of multilayered magnetic films and granulated magnetic systems. The maximal value of the relative magnetoresistance $\delta_H = [\rho(H) - \rho(0)]/\rho(H)$, taken at a field strength of $H = 6$ T, was found in Fe–Cr films at 4.2 K: it amounted to -150% [1].

This direction may turn out to be nonoptimal, as there exist room-temperature magnetic semiconductors with giant magnetoresistance (GMR), by many orders of magnitude exceeding that of multilayered films and granulated systems. For example, in $La_{0.67}Ca_{0.33}MnO_y$ films the relative magnetoresistance δ_H amounting to -127000% at 77 K and to -1300% at room temperature was found [2]. Certainly, these values greatly exceed those obtained for multilayered films and granulated systems, but they do not reach the upper bound for the GMR which can be achieved in heavily doped magnetic semiconductors. The champion is the heavily doped antiferromagnetic EuSe semiconductor in which at liquid-helium temperatures quite fantastic values of δ_H of order $-10^{11}\%$ have been observed [3]. But in the La–Ca–Mn–O system the magnetoresistance at 57 K can reach a value of order $-10^8\%$ which is very impressive, too [4].

Quite recently, the fact that the magnetic semiconductors are very promising was, at last, recognized. Massive investigations began on such magnetic semiconductors as lanthanum

E L Nagaev Institute for High Pressure Physics,
Russian Academy of Sciences,
142092 Troitsk, Moscow Region, Russia
Fax (7-095) 34-00 12; E-mail: tsir@elch.chem.msu.su

Received 27 February 1996, revised 22 April 1996
Uspekhi Fizicheskikh Nauk **166** (8) 833–858 (1996)
Translated by E L Nagaev, edited by A Radzig

manganites and related compounds, which are especially promising for technical applications. An evidence for it is a sharp rise in the number of publications on the subject in scientific journals withi in 1995 (only in Physical Review Letters the number of publications for this year exceeded by an order of magnitude their total number for the preceding decade) and a literal boom about lanthanum manganites at the 40th Conference on Magnetism and Magnetic Materials (Philadelphia, November 1995) [4 – 31].

In this article a review will be given of crystallographic, magnetic and electric properties of the lanthanum-based perovskites and related materials. Though one often denotes their high-conductive ferromagnetically ordered state as a metallic one, in actual fact their conductivity is several orders of magnitude lower than that for common metals, being typical of degenerate semiconductors in their order of magnitude. Taking additionally into account the fact that the basic material ($LaMnO_3$) for high-conductive compounds is a semiconductor, it seems quite natural to classify these materials as degenerate ferromagnetic semiconductors. For this reason a theory of ferromagnetic semiconductors will be also presented, which enables the properties of these materials to be explained. This theory is formulated in terms more general than it is necessary for the concrete class of materials which initiated the present article. Respectively, one may also consider this work as a review article on general properties of degenerate ferromagnetic semiconductors.

2. Crystallographic properties of lanthanum manganites

The basic material for degenerate ferromagnetic semiconductors of the class under consideration is $LaMnO_3$. If one replaces La by a bivalent metal, for example, Ca, in the latter, then in the limiting case of the complete substitution it goes over into $CaMnO_3$. Both these materials have the perovskite structure [32, 33]. The structure of an ideal cubic perovskite ABO_3 may be conceived as a set of regular octahedrons BO_3, which make contact with each other by their vertices [34, 35]. Here A is the large cation which occupies the centre of the cubooctahedron, B is the small cation occupying the centre of the octahedron. At the vertices of the polyhedrons, the oxygen ions are located. In the case of $LaMnO_3$ the large cation is La^{3+} of 122 pm radius, and the small one Mn^{3+}, 70 pm in radius. The Ca^{2+} radius forms 106 pm and the Mn^{4+} radius, 52 pm [36].

Compounds of cubic perovskite structure are met seldom. The crystalline lattice is normally distorted in some way. The distortions can be grouped as follows: (1) those caused by discrepancy between sizes of cations and pores which they occupy; (2) those caused by the Jahn–Teller effect [35, 37]. In the first case the minimum of the free energy is achieved by rotation of the BO_6 octahedrons about one of the axes or about several axes of the initial lattice. If the octahedrons rotate about the [100] axis, a tetragonal distortion takes place, if they do about the [110] axis, the orthorhombic one ($a \neq b \neq c$, $\alpha = \beta = \gamma = 90°$), and about the [111] axis, the rhombohedral one.

In the second case the distortion is caused by the fact that the Mn^{3+} ion entering the manganites considered, is degenerate with respect to d-orbitals in a cubic field: the latter splits the atomic d-level into the twofold degenerate e_g and threefold degenerate t_{2g} levels. The former lies higher than the latter, so that four d-electrons of the Mn^{3+} ion fill the t_{2g} level completely, and the e_g level only partially. This is the cause for the cooperative Jahn–Teller effect which reduces the energy of such a degenerate system by lowering its symmetry, which in turn lifts the degeneracy of the electronic levels.

Several investigators tried to establish which of the two sublevels corresponding to the e_g level goes down due to the Jahn–Teller effect. This was discussed in detail in Ref. [38], where conclusion was made that in the orthomanganites the ground state of an e_g-electron is the d_{z^2}-sublevel. Such orbitals display the antiferrodistorsional ordering which manifests itself in the O'-orthorhombic structure of the crystal.

Somewhat different results were obtained by other researchers. According to Refs [39, 40], the $La_{1-x}Ca_xMnO_3$ structure at $x = 0$ and 300 K is monoclinic. On increase in x, it goes over first to the orthorhombic one (near $x = 0.05$) and then to the cubic one (near $x = 0.15$). In the monoclinic phase the angle between a and b axes differs from 90° less than by 1°. At $x \neq 0$, the temperature rise causes transitions of the monoclinic phase into the orthorhombic one and of the orthorhombic phase into the cubic one. But it was concluded in Ref. [41] that the $LaMnO_3$ structure below 875 K represents a strongly distorted orthorhombic phase. According to Ref. [42], the $La_{1-x}Sr_xMnO_3$ structure is orthorhombic at x less than 0.175. At larger x it is rhombohedral (Fig. 1).

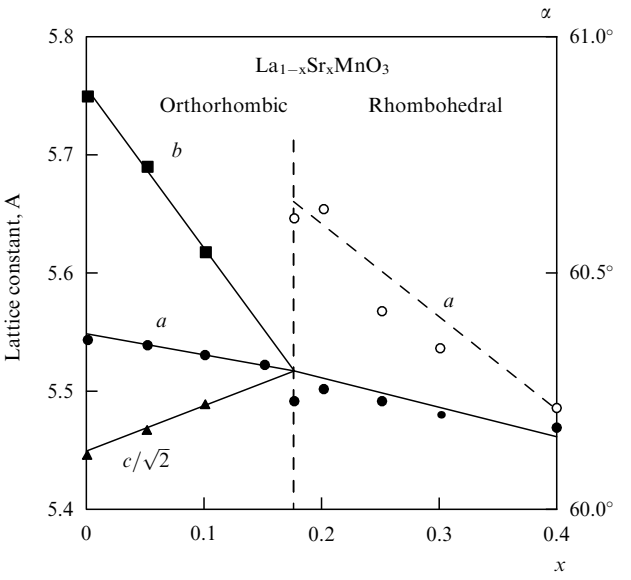

Figure 1. Lattice constants of $La_{1-x}Sr_xMnO_3$ at 300 K [42].

According to Ref. [38], the O'-rhombohedral phase realizes in $La_{1-x}Ca_xMnO_3$ at small x, like in pure $LaMnO_3$. The $La_{1-x}Ca_xMnO_3$ phase diagram at x less than 0.15 is characterized by a wide range of coexistence for O- and O'-orthorhombic phases. On rise in temperature, the O'-phase is replaced continuously by the O-phase. At $x = 0.4$ an additional phase transformation occurs, the nature of which is not yet established (Fig. 2).

Theoretical papers [43, 44] have been devoted to the structure and energy band spectrum of the crystals under consideration. In them the local spin density approximation is used. In Ref. [44] the importance was stressed of accounting for the distortion of cubic structure: only this makes it possible to describe correctly the magnetic structure and insulating state of $LaMnO_3$. A similar conclusion was made in Ref. [15]:

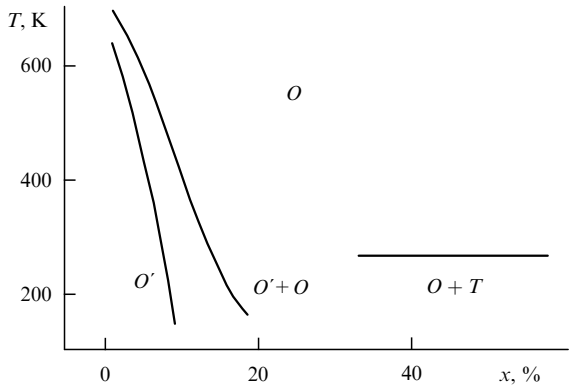

Figure 2. Crystal-structure phase diagram of $La_{1-x}Ca_xMnO_3$. The *O* and *O′* phases are defined in the text. The *T* phase is not identified uniquely.

in order to obtain the gap at the Fermi surface, one should account for the lattice distortion due to the Jahn–Teller effect. Like in Ref. [43], in the latter work a considerable degree of the Mn(d) — O(p) hybridization was also found.

3. Magnetic properties of lanthanum manganites

3.1 Unsubstituted lanthanum manganites

The magnetic structure of $LaMnO_3$ was established by neutronographic investigations in [34]. It is represented by an antiferromagnetic lattice consisting of ferromagnetic layers of Mn ions. But the alternating (100) planes have opposite spin directions. If one chooses the antiferromagnetism vector as the *z* axis, then the moments should lie in the *xy*-plane or very close to it.

According to [40], the Néel temperature T_N of this material equals 141 K, and it displays weak ferromagnetism due to the Dzyaloshinskii field. Though this weak ferromagnetism may be easily confused with that appearing as a result of nonstoichiometry of the sample, there are evidences that it really exists in this case: in highly perfect samples the spontaneous magnetization vanishes at just the same temperature at which the susceptibility displays a kink typical of antiferromagnetic systems. An additional evidence is the hysteresis along the magnetization axis occurred on cooling the sample and typical of the weak ferromagnets.

In Ref. [34], the magnetic structure of $CaMnO_3$ with $T_N = 131$ K was determined. In this material each Mn^{4+} ion is surrounded by 6 neighbouring Mn^{4+} ions with spins antiparallel to the spin of the ion given. Such a structure may be represented as two interpenetrating face-centred cubic lattices with the opposite spin directions. The same structure realizes also in $SrMnO_3$ with $T_N = 260$ K.

3.2 Substituted manganites: the canted antiferromagnetism or ferro-antiferromagnetic phase separation?

As was established in Ref. [45], replacement of the trivalent La ions by the bivalent Ca, Ba, or Sr ions leads to appearance of spontaneous magnetization in the $LaMnO_3$ crystals. At small doping *x* it is nonsaturated, and becomes saturated only at $x = 0.3$. In the vicinity of $x = 0.5$, the magnetization sharply disappears again, which seems quite natural: as has been already pointed out $CaMnO_3$ is antiferromagnetic (Fig. 3).

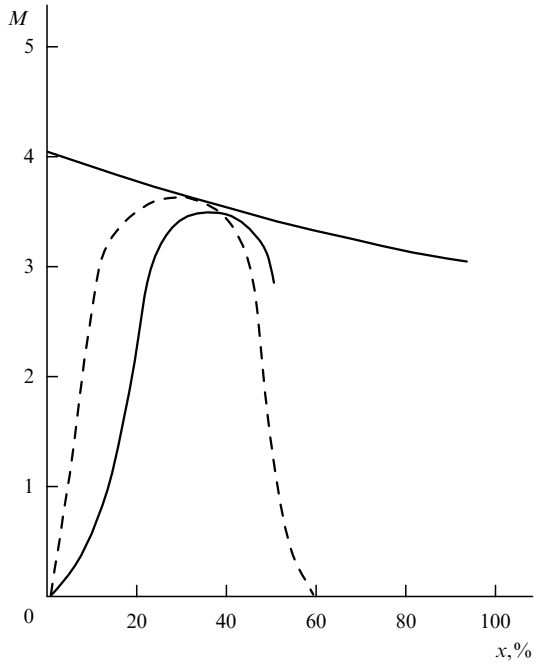

Figure 3. Dependence of the magnetization *M* for the $La_{1-x}Ca_xMnO_3$ system on *x* (in arbitrary units) The solid line is from Ref. [34], dashed line — from Ref. [45]. The upper line shows the saturation magnetization.

The nature of the nonsaturated magnetized state in $La_{1-x}Ca_xMnO_3$ was elucidated in Ref. [34] by neutronographic studies of this compound. In the *x* range whereat the complete ferromagnetic ordering is absent, the neutron scattering spectra at 4.2 K constitute a superposition of spectra corresponding to both the ferromagnetic and antiferromagnetic orderings. In Figure 4, the spectrum of a sample with $x = 0.18$ is presented. The antiferromagnetic peaks are shaded, the remaining peaks are ferromagnetic.

Principally, such spectra may be related both to the two-phase state of the sample, when it is a mixture of the ferromagnetic and antiferromagnetic regions, and to a single-phase two-sublattice state with the nonzero total

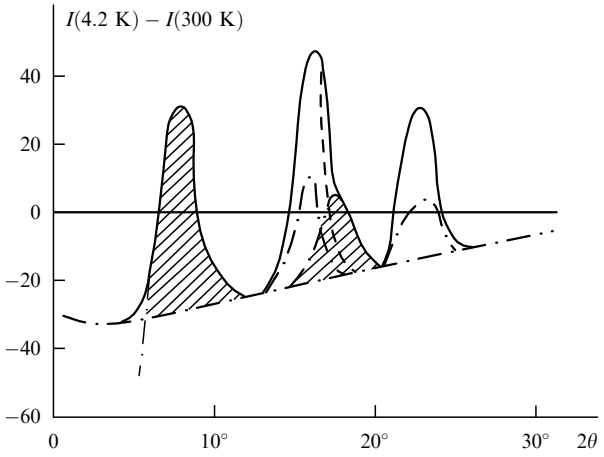

Figure 4. Neutron scattering intensity (in arbitrary units) vs. scattering angle 2θ in $La_{1-x}Ca_xMnO_3$ with $x = 0.18$ at 4.2 K minus the intensity at 300 K. Shaded peaks are antiferromagnetic, unshaded — ferromagnetic. Dashed lines depict the same spectrum taken in the 4.5 kOe field [34].

moment. As examples of the latter, the canted antiferromagnetic state or collinear state of the ferrimagnetic type may be pointed out.

A unique choice between the two-phase state and single-phase state may be done by investigating the neutronographic spectra dependence on the external magnetic field. If the field is aligned with the unit neutron-scattering vector $\mathbf{q}$, then the ferromagnetic peaks must become lower and disappear at all in the high-field limit. This follows from the fact that the intensity of the ferromagnetic scattering I_{FM} is proportional to $\left[1-(\mathbf{q}\cdot\mathbf{m})^2\right]$, where $\mathbf{m}$ is the unit vector aligned with the magnetic moment (see, for example, Ref. [46]). The stronger is the field, the closer is the direction of $\mathbf{m}$ to the field $\mathbf{H}$ and the less is the intensity I_{FM} which vanishes at $H\to\infty$.

On the other hand, the intensity of the antiferromagnetic scattering I_{AF} is proportional to $\left[1-(\mathbf{q}\cdot\mathbf{l})^2\right]$, where $\mathbf{l}$ is the unit vector aligned with the difference between the moments of the sublattices. If the system is phase-separated, then the vectors $\mathbf{m}$ and $\mathbf{l}$ are not coupled, and the magnetic field of a strength less or comparable to the anisotropy field H_{A} will rotate only the vector of magnetism $\mathbf{m}$, not affecting the vector of antiferromagnetism $\mathbf{l}$. Really, if the field is aligned with the anisotropy axis, then the vector $\mathbf{l}$ changes its orientation abruptly only at the sufficiently large field strength — of order $(H_{\mathrm{A}}H_{\mathrm{E}})^{1/2}$, where H_{E} is the exchange field (see, for example, Ref. [47]). Thus, at weak fields the antiferromagnetic scattering should not change.

But, if the system is single-phase, the vector $\mathbf{m}$ will rotate together with the vector $\mathbf{l}$, and for this reason, if the ordering is ferrimagnetic ($\mathbf{m}\|\mathbf{l}$), then the antiferromagnetic scattering should also be reduced, and, if the ordering is canted antiferromagnetic ($\mathbf{m}\perp\mathbf{l}$), it should be enhanced.

Figure 4 shows clearly that a magnetic field of 4.5 kOe reduces the ferromagnetic scattering by more than a half and has no effect whatsoever on the antiferromagnetic scattering. Hence, one may conclude that the crystal is in the two-phase ferro-antiferromagnetic state.

Unfortunately, these conclusions of Ref. [34] were ignored by de Gennes in his paper [48] where appearance of the spontaneous magnetization in manganites was ascribed to the canted antiferromagnetic ordering. Since then this erroneous version was repeated by many authors. Meanwhile, it contradicts not only the neutronographic data but also the electric data. Really, according to Ref. [48] the canted antiferromagnetic ordering may appear only as a result of charge carrier delocalization, i.e. of their free motion over the crystal. This means that the crystal should be high-conductive. But in actual reality, at $x<0.15$ a crystal with an unsaturated magnetization behaves at $T=0$ like an insulator [49] (see Section 5.1).

It should be added that there exist experimental data (see below Section 5.1) according to which the double exchange between the Mn ions (on which the theory [48] is based) in actual conditions is absent in manganites as the charge carriers (holes) move not over the Mn ions but over the oxygen ions.

Meanwhile, quite recently FMR (ferromagnetic resonance) experimental data were obtained which confirm the fact that the epitaxial $A_xB_{1-x}MnO_{3-y}$ manganite films (A = La, Nd; B = Ca, Sr, Ba) are in an inhomogeneous state: they consist of high-conductive regions with the resistivity less than 10^{-2} Ohm cm, and low-conductive regions with the resistivity 100 times or more higher [30].

Recently it was also confirmed that in the $R_{0.67}Sr_{0.33}MnO_z$ films (R = Nd, Pr) with the oxygen deficiency there exist ferromagnetic microregions with diameter from 7 to 10 nm below 30 K [10]. These spin clusters give rise to appearance of superparamagnetic properties in these films which manifest themselves: (1) in enhanced difference between magnetizations measured on sample cooling with or without magnetic field; (2) in drastic falling of the latter quantity at low temperatures; (3) in strongly enhanced value of the paramagnetic Curie temperature as compared with the magnetic ordering temperature; (4) in sharp falling of the coercive force with increasing temperature at its low values.

Still earlier it was established [39, 40] that at small doping x the paramagnetic Curie temperature Θ of the La–Ca–Mn–O system sharply increases on increase in x. But the Néel temperature remains practically unchanged. The author of Refs [39, 40] pointed out with good reason that this evidences existence of ferromagnetic regions inside the crystal which do not interact with each other. Really, as was shown in Refs [50, 47], if a semiconductor is nondegenerate, then magnetized microregions arise in the vicinity of un-ionized donors or acceptors. They enhance strongly Θ but do not affect virtually T_{N}. The constancy of T_{N} established in papers [39, 40] evidences that the magnetic ordering in the main part of the crystal remains collinear antiferromagnetic (neglecting the inherent weak ferromagnetism), though in [39, 40] it was considered as canted antiferromagnetic with the moment enhancing with the hole density.

It should be pointed out that other magnetic investigations exist, the data of which cannot be certainly explained in terms of the canted antiferromagnetic ordering, but can be possibly explained by the phase separation. For example, NMR study on ^{55}Mn [39, 40] yields that at $x<0.175$ the spectrum consists of two parts, and for samples with $x=0.2$ and 0.3 it is specified by the sole part. The latter is identified with a line narrowed due to the translational motion of charge carriers over the Mn ions and for this reason is related to the high conductivity of these samples. If so, then the question still remains to be answered why two peaks arise in the region of the assumed canted antiferromagnetic ordering. This region should just appear as a result of the translational motion of the carriers over the crystal and therefore its properties should be of the same type as those of the ferromagnetic region.

Quite similarly, it is rather difficult to explain results of the NMR studies on ^{139}La nuclei [51] in which a large field was observed on them in $La_{0.9}Na_{0.1}MnO_3$ even after disappearance of the crystal magnetization (this work develops studies carried out in [52]). In conclusion, it should be said that there are also theoretical objections to the canted antiferromagnetic ordering. As will be pointed out in Section 6.8, such a state in an antiferromagnetic semiconductor with the double exchange, first, can be energetically more favoured than the collinear structures only at charge carrier densities large enough and, second, it is unstable against electrostatic fluctuations which make the crystal go over into a nonuniform state. What exactly is the nature of this nonuniform state, one can conclude only after detailed theoretical study of the problem. In particular, it may correspond to the separation into the ferromagnetic regions in which all the charge carriers are concentrated, and collinear antiferromagnetic regions without charge carriers (the electron phase separation, see Section 4.1).

3.3 Ferromagnetic state of the substituted lanthanum manganites

At sufficiently heavy doping (between $x = 0.2$ and 0.6, see Fig. 3) the $La_{1-x}D_xMnO_3$ compounds become completely ferromagnetic and corresponding Curie points T_C essentially depend on their compositions. For example, for D = Ca with $x = 0.3$ the Curie point is 250 K [39]. For D = Sr in the range from $x = 0.25$ to 0.5 the Curie temperature is virtually x-independent, being close to 350 K [42], and for D = Pb it attains the maximum value of 370 K at $x = 0.4$ [53].

Completely ferromagnetic materials may also be fabricated without doping through the production of nonstoichiometric compositions. Thus, $LaMnO_{3.11}$ is a ferromagnet with T_C of about 160 K [54, 55]. The ferromagnetism can be brought into existence also by the La deficiency: epitaxial thin $La_{1-x}MnO_{3-y}$ films deposited on the $SrTiO_3$ substrate are ferromagnetic already at $x = 0$. But, on increase in the La deficiency, the Curie point of as-grown films increases from 135 K at $x = 0$ to 265 K at $x = 0.33$. Annealing in the oxygen atmosphere raises the Curie point almost up to room temperature [9, 56].

Investigations of the T_C dependence on the pressure P carried out on $La_{1-x}Sr_xMnO_3$ single crystals [57] yielded that in the range $0.15 \leqslant x \leqslant 0.5$ the Curie temperature T_C increases with pressure. But the shift of T_C depends on x: the quantity $d \ln T_C / dP$ amounts to 0.065 GPa^{-1} at $x = 0.15$ and only to 0.005 GPa^{-1} at $x = 0.4-0.5$.

In Ref. [20], magnetically uniform $La_{0.67}Ba_{0.33}MnO_3$ films were investigated as being in the completely ferromagnetic state. At low temperatures the magnetization reduces with increasing temperature according to the Bloch $T^{3/2}$-law. This gives evidence that magnons are the well-defined elementary excitations in them.

As shown in Ref. [58], on increase in x, the concentration phase transition from the ferromagnetic state to the antiferromagnetic one occurs discontinuously in $La_{1-x}Ca_x$ at $x = 0.5$. Magnetization of the $x = 0.5$-compound at $T \to 0$ in a magnetic field of 1 T is small and does not change essentially up to 200 K. But, on further increase in T, the magnetization reaches a strongly pronounced maximum about 220 K and then falls down as should be the case in the paramagnetic state. At the reverse temperature change, after reaching 220 K, the magnetization continues to grow almost down to 170 K, and then decreases sharply. The hysteresis loop becomes closed at about 125 K. In addition to the magnetization hysteresis, the resistivity hysteresis was also found to exist in this sample.

The magnetization behaviour just described makes it clear that at low temperatures this material is antiferromagnetic, but with increase in temperature it displays the first-order phase transition into the ferromagnetic state. This transition is characterized by a very wide hysteresis loop. The fact of the ferromagnetic state existence at elevated temperatures is confirmed by the virtual magnetization saturation in a field of 2 T, when the magnetization reaches 70% of maximally possible value. The antiferromagnetic ordering at low temperatures was established by neutronographic studies of this material.

Experimental data now available give evidence to an anomalously strong coupling between the magnetic subsystem and lattice in lanthanum manganites. For instance, in Ref. [59] an anomalously large thermal lattice expansion was found in $La_{0.60}Y_{0.07}Ca_{0.33}MnO_3$ with a peak at the Curie point T_C, which was suppressed by an applied magnetic field.

The magnetic-lattice coupling is especially clearly pronounced at some specific degrees of doping. For instance, according to Refs [39, 40], the $La_{1-x}Ca_xMnO_3$ cooling in a magnetic field from room temperature to the liquid nitrogen temperatures leads to appearance of marked induced anisotropy in a narrow range of the x variation close to 0.175. This may point to dependence of the cooperative Jahn–Teller effect on the magnetic ordering.

According to Ref. [60], the crystalline structure may be changed in $La_{1-x}Sr_xMnO_3$ with $x = 0.17$ by a magnetic field from orthorhombic to rhombohedral ones — at low temperatures irreversibly, and at elevated temperatures reversibly. It should be noted that this x value just corresponds to the transition from the semiconducting to the metallic conductivity at low temperatures [42, 49].

Another specific point falls at $x = 0.5$, where the crystal makes choice between the antiferromagnetic ordering and the ferromagnetic one. On decrease of temperature below T_C, the Jahn–Teller effect takes place in $La_{1-x}Ca_xMnO_3$, which manifests itself in a sharp decrease of the lattice constant along the b axis and its increase along the a and c axes. But the volume of the unit cell does not change in the process. A lattice distortion at T_C itself with a sharp decrease in all the lattice constants was observed at $x = 0.25$. The relative change in the crystal volume reaches there a very large quantity of 0.13%, which was related by the authors to a change in conductivity type at the Curie point [61].

In Ref. [62], when analyzing data of magnetic measurements on the crystals of the system under consideration, the conclusion was made that the indirect exchange in this system is described by the RKKY theory quite satisfactorily. When this paper was published, such a conclusion was treated as paradoxical, as if the holes are in the states of the Mn^{4+} type, the applicability conditions for the RKKY theory are not met certainly. But recent results already mentioned above (see also Section 5.1) according to which the holes move over the oxygen ions make this situation quite realistic. If the holes really correspond to the Mn^{4+} ions, then the indirect exchange in such a system should be described with the aid of a theory developed in Refs [63, 47] (partly it is presented in Section 6.6).

4. Giant magnetoresistance at ferro-antiferromagnetic phase separation and at charge ordering

Before analyzing the nature of the phase separation in lanthanum manganites, it is advisable to analyze the phase separation as a physical phenomenon in general. First, it should be pointed out that there exists a trivial inborn phase separation caused by inhomogeneity of the chemical composition of a sample, for example, due to the nonuniformity of the impurity distribution over a sample, which arises at the moment of its synthesis at elevated temperatures and remains frozen after its cooling. Such a phase separation is not sensitive to external factors (temperature or magnetic field) and for this reason it is an individual property of each concrete sample.

But a nontrivial thermodynamically equilibrium phase separation also occurs which is changed under external factors, and for this reason it is controllable. Two mechanisms of such a reversible phase separation are known in degenerate magnetic semiconductors: the electronic phase separation occurring at frozen impurity positions [47, 64 –

66], and magnetoimpurity phase separation occurring through the impurity atom diffusion [65 – 69]. Both these mechanisms are related here to the fact that the ferromagnetic ordering is more energetically favoured for charge carriers than the antiferromagnetic one [47]. For this reason they tend to establish the ferromagnetic ordering. But, in order to realize this in an entire crystal, the carrier density must be sufficiently high. If it is insufficient for this aim, all the carriers may concentrate in a portion of the crystal and establish there the ferromagnetic ordering. The remaining part of the crystal is antiferromagnetic and insulating.

4.1 Electronic phase separation. Record magnetoresistance

In the case of electronic phase separation, concentration of the charge carriers in a portion of the crystal, where they cause appearance of the ferromagnetic ordering, leads to the mutual charging of both the phases. This is a consequence of the fact that the ionized donor or acceptor impurity with the charge opposite to that of the charge carriers, unlike them, is distributed uniformly over the crystal. Thus, strong Coulomb fields arise which tend to intermix regions of the ferromagnetic and antiferromagnetic phases and thus to lower the Coulomb energy of the system involved.

At relatively small carrier densities, the high-conducting ferromagnetic regions form separated, not making contacts with each other, droplets inside the insulating antiferromagnetic host (Fig. 5a). As they are separated from each other by the insulating layers, the crystal as a whole is an insulator at $T = 0$ (if one neglects the tunnel currents flowing between droplets).

On increase in the carrier density, the volume of the ferromagnetic phase also increases and, beginning from a certain critical density n_p, the ferromagnetic droplets begin to make contacts with each other, i.e. percolation of the ferromagnetic ordering, as well as of the charge carrier liquid, occurs. This means that the concentration insulator-to-metal transition takes place. On further increase in density, the geometry of the two-phase state changes drastically: the ferromagnetic region transforms from multiply-connected to simply-connected. In other words, the ferromagnetic portion of the crystal consists of separated droplets inside the ferromagnetic host (Fig. 5b). And lastly, at still more higher carrier density, the entire crystal becomes ferromagnetic.

Such an electronic phase separation realizes in heavily doped antiferromagnetic EuSe and EuTe semiconductors (see experimental verification of this statement in Refs [47, 65, 66]). In particular, it leads to a supergiant magnetoresistance rather than to a magnetoresistance which one uses to call as giant. Especially pronounced is this effect in EuSe, which is an isotropic metamagnetic system with a very weak field of transition from the antiferromagnetic state to a ferromagnetic one [3, 47]. At the mean conduction-electron density somewhat below 10^{19} cm^{-3}, the main portion of the crystal is antiferromagnetic at temperatures below 5 K, and all the conduction electrons are concentrated on separated ferromagnetic droplets (the configuration of Fig. 5a). The resistivity of such a crystal exceeds 10^7 Ohm cm.

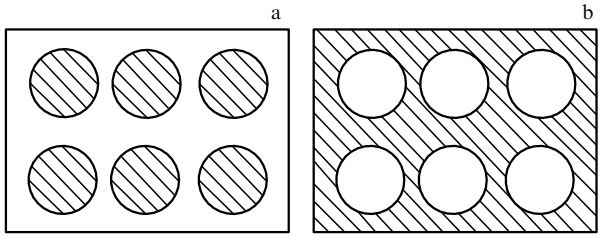

Figure 5. The phase-separated state of a degenerate antiferromagnetic semiconductor: (a) insulating state; (b) conducting state (hatched is the ferromagnetic part and nonhatched is the antiferromagnetic part of the crystal) [64].

But already a magnetic field of 10 kOe reduces the resistivity to 10^{-2} Ohm cm, i.e. by 9 orders of magnitude (Fig. 6a). This happens due to the transition of the entire crystal into the ferromagnetic state. As a result, the conduction electrons that were locked inside the droplets spread over the entire crystal. Evidently, in this case the absolute record of the isotropic negative magnetoresistance is achieved ($\delta_H \sim -10^{11}$ %). In the case of the configuration in Fig. 5b, realized at larger electron densities, both the resistivity and magnetoresistance are typical of a degenerate ferromagnetic semiconductor: the resistivity displays a peak in the vicinity of T_C, and a field of 10 kOe reduces the peak by a factor of 5 (Fig. 6b). The insulator-to-metal transition in a field displayed in Fig. 6a is of the same type as that presented in Fig. 7.

The giant magnetoresistance of the phase-separated EuTe with the geometry of Fig. 5a manifests itself already in weak fields: a field of less than 200 Oe reduces the resistivity of a sample by half at 4.2 K [70]. The effect can be explained as follows: the magnetic field increases the size of ferromagnetic droplets and, hence, it facilitates the electron tunnelling between droplets.

In addition, the field aligns moments of droplets which also facilitates tunnelling. At last, the field tends to destroy the ferromagnetic droplets [47]. For this reason it increases the energy of electrons trapped in the droplets and diminishes the energy of their delocalization (transition to the conduction band of the antiferromagnetic portion of a crystal). The tunnel transitions and magnetoresistance related to them do not vanish even at $T = 0$.

It should be stressed that such a phase-separated state is the crystal ground state, and it is destroyed by the rise in temperature. Then the crystals which were in the insulating state of the Fig. 5a-type at $T = 0$ go over into the high-conductive state as the insulating regions cease to exist.

4.2 Impurity phase separation

An alternative to the electronic phase separation is the magnetoimpurity phase separation which is caused by two factors simultaneously:

(1) Interaction between impurity donor or acceptor atoms resulting in the formation of an 'impurity metal', which consists of them. In other words, delocalization of the charge carriers occurs according to the well-known Mott mechanism. In full analogy with the conventional metal, the tendency appears to establish such an interatomic spacing which provides the minimum to the total energy of the system. If the mean impurity density over the crystal is less than this optimal density, then it is energetically favoured for the impurity atoms to concentrate in a certain portion of the crystal. Then the remaining part of the crystal will not contain them at all.

(2) The same tendency of charge carriers to establish the ferromagnetic ordering, as at the electronic phase separation, makes the electrons or holes to assemble together in a portion of the crystal where they establish jointly this ordering. But,

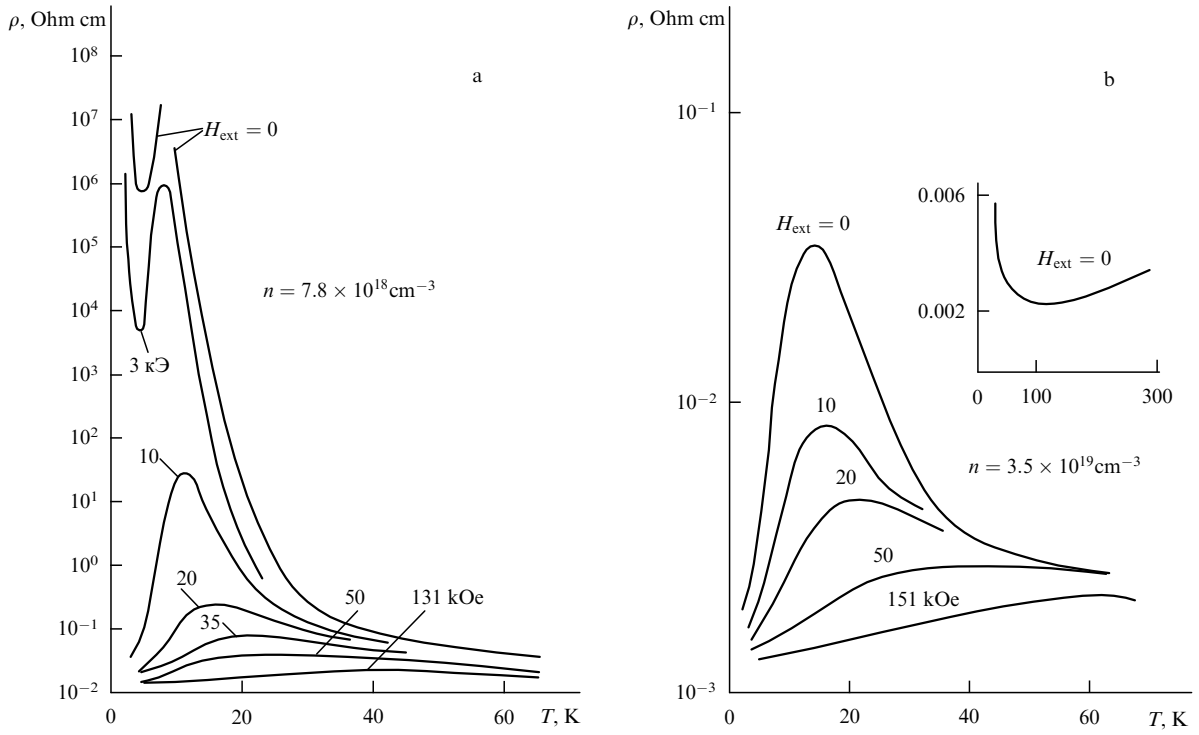

Figure 6. Resistivity ρ in different fields H_{ext} vs. temperature T for EuSe specimens with two charge-carrier concentrations n at 297 K [3].

along with them, in one or another area of this portion the 'parent' impurity atoms also assemble.

An essential difference between the impurity phase separation and the electronic phase separation is the absence of the mutual charging of the phases at the former, as the electron or hole charges are compensated for the charges of impurity ions diffusing together with carriers. As a result, the ferromagnetic regions can be sufficiently large in size even at small carrier densities. But here the region size is limited by the elastic forces which do not allow, for example, a crystal of a macroscopic size to be separated only into two regions of different phases. For this reason, on increase in the carrier density, the topology of the high-conducting ferromagnetic portion should change here at a certain percolation density n_p, which occurs jointly with the concentration phase transition from the insulating state to the high-conductive one.

In principle, at the impurity phase separation the magnetic field should also increase the size of the ferromagnetic regions, thus facilitating the electron tunnelling between them. Hence, the very fact of the phase separation serves here as one of the possible mechanisms of negative magnetoresistance, too.

On increase in temperature, the phase-separated state should be broken, and the impurity distribution over the crystal should become uniform. Thus, the mean impurity density will be less than the local density in impurity-rich regions. Meanwhile, the delocalization of electrons belonging to the donor impurity or holes belonging to the acceptor impurity can take place only at sufficiently large impurity densities. Hence, the situation is possible principally, when, on destruction of the insulating impurity-phase-separated state of the Fig. 5a-type, the crystal does not go over into the high-conductive state. Actually, if the impurity density in the impurity-rich regions was sufficiently large for the electron (hole) delocalization, the mean density may turn

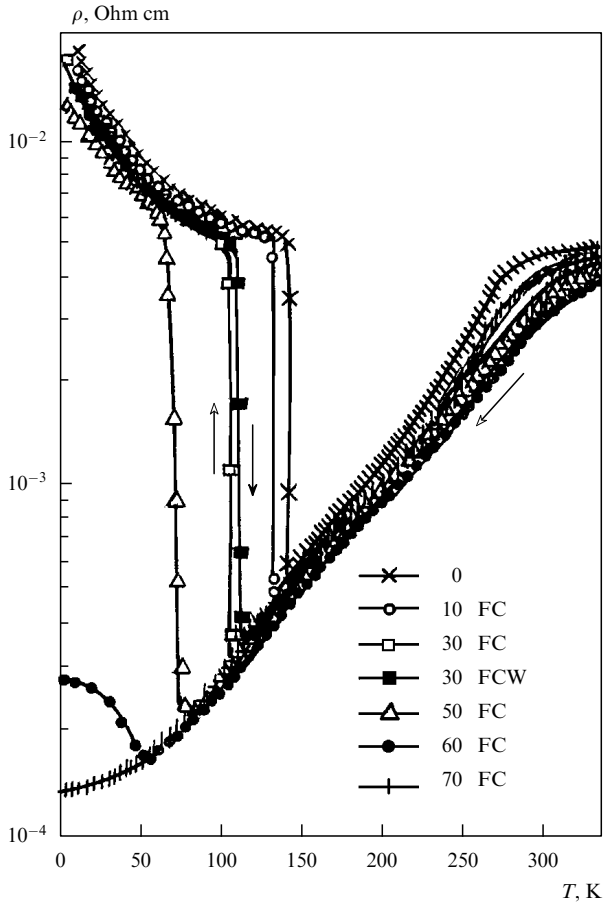

Figure 7. Temperature-dependence of resistivity of $Pr_{0.5}Sr_{0.5}MnO_3$ in a magnetic field. Results are obtained on sample cooling from 330 K to 4.2 K in the corresponding magnetic fields (in kOe). For a 30 kOe field, both the curves are presented which correspond to the cooling in the field (FC) and to the heating of samples cooled in the field (FCW) [73].

out to be insufficient for this aim after destruction of the phase-separated state.

The mean impurity density may also be sufficient for the metallization, though, and then destruction of the phase-separated state will lead to the crystal transition to the high-conductive state. In the case of the Fig. 5b-type geometry, destruction of the phase-separated state does not change the metallic type of the conductivity.

Certainly, in order to realize the impurity phase separation, the impurity-atom diffusion coefficient must be sufficiently large at actual temperatures. There is direct experimental evidence that the oxygen diffusion coefficient is high in many perovskites: at room temperatures it may reach values of the order of 10^{-9} cm^2 s^{-1}, which ensure oxygen rapid diffusion at these temperatures. Moreover, in the $La_2CuO_{4+\delta}$ perovskite the crystal separation into the oxygen-rich and oxygen-poor regions occurs even at 265 K . There exist many other HTSCs in which the impurity phase separation was discovered (see Refs [65, 66]).

4.3 Nature of phase separation in the substituted lanthanum manganites

Now let us discuss the nature of the phase-separated state in the lanthanum manganites. As was pointed out in Ref. [34], both the phases involved do not differ in their crystallographic structure. Thus, they should differ either in the impurity content, or in the charge carrier density. Furthermore, the formation of the ferromagnetic phase is unlikely to be ascribed to appearance of the Mn^{4+} complexes inside it, for the exchange between them is antiferromagnetic. This can be inferred from the antiferromagnetic ordering in $CaMnO_3$. The enhanced number of charge carriers does not imply yet an appearance of such ions. If the holes really move over the Mn ions (but this is questioned now, see Ref. [71] and Section 5.1), this means that the Mn ions are in a uniform state with the valency intermediate between 3 and 4. For this reason the claim made in Ref. [16] seems to be very strange. The authors argue that the electronic phase separation for Mn^{3+} and Mn^{4+} ions is discovered which should lead to a nonuniform mixed-valency state.

Further, one may conclude unambiguously that the ferromagnetic phase is high-conductive, and the antiferromagnetic phase — insulating. This is obvious from comparison of the data on the $La_{1-x}Sr_xMnO_3$ conductivity [42, 49] which are close to each other (see Fig. 8), and data on the magnetization of the same material [34, 49] (they resemble closely those in Fig. 3). Evidently, in the range where the magnetization is small and the main portion of the crystal is antiferromagnetic, it behaves like an insulator. But, when its magnetization becomes high, the conductivity is high, too.

Using the data from the preceding section, according to which at small x the ferromagnetic regions occupy the smaller portion of the crystal, one should infer that here the situation is realized which corresponds to Fig. 5a, i.e. to the insulating state. On increase in x, independently of the nature of the phase-separated state, the percolation of the hole liquid and ferromagnetism should occur with appearance of the topology as in Fig. 5b. Hence, the samples should go over into the high-conductive state still before reaching the complete magnetization. Just this was found experimentally (compare Figs 3 and 8). As was already pointed out, such a concentration insulator-to-metal phase transition cannot be explained within the framework of the canted antiferromagnetism hypothesis.

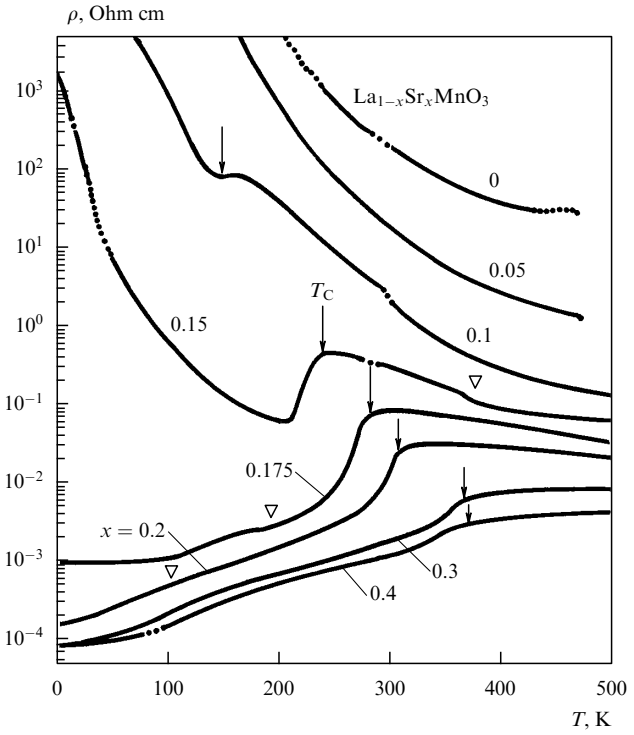

Figure 8. Temperature dependence of resistivity for $La_{1-x}Sr_xMnO_3$ crystals. The arrows denote the Curie points. Anomalies denoted by light triangles are related to structural transformations [42].

Unfortunately, the mechanism of the phase separation in lanthanum manganites remains unclear. If one assumes that it is electronic, then the following facts should be explained: (1) on increase in temperature, in the resistivity vs. temperature curves a sharp transition from the low-conductive state to the high-conductive one is absent, which is typical of the electronic phase separation with the Fig. 5a geometry; (2) regions of both the phases are so large that they yield well-defined neutron scattering peaks observed in Ref. [34]. (Fig. 4). In the case of the electronic phase separation, far from the percolation density n_p, the droplet size of the smaller-volume phase is small, so that the droplets cannot produce the well-defined peaks and can only produce the small-angle neutron scattering.

The answers to these questions may be as follows. First, studies of the manganite conductivity were carried out up to not very high temperatures, and the insulator-to-metal transition may exist at higher temperatures. Second, in the vicinity of the percolation density, to which the Fig. 4 corresponds, the regions of both the phases can be large in size. For this reason a more detailed experimental investigation of these materials is necessary.

An indirect evidence for the electronic phase separation is an anomalously large magnetoresistance of the La–Ca–Mn–O system in the range of dominating antiferromagnetic ordering found in Ref. [4]: it is several orders of magnitude larger than the magnetoresistance of the completely ferromagnetic materials. Magnetoresistance δ_H values of $-830\,000\%$ at 125 K and $-10^8\%$ at 57 K were achieved. The latter is only 3 orders of magnitude lower than the record magnetoresistance of EuSe.

As for the hypothesis of the reversible impurity phase separation, this phenomenon can be hardly realized with

participation of a bivalent dopant. For example, it is difficult to expect that the diffusion coefficient for Ca is high as its atomic radius is large, amounting to 197.3 pm. But the oxygen atomic radius is considerably less, amounting to only 66 pm [36]. For this reason a hypothesis may be advanced that introduction of Ca ions into $LaMnO_3$ may lead to the impurity phase separation with respect to the oxygen [72a].

Then the oxygen-rich regions should be characterized by an enhanced charge carrier density as both the excess oxygen and Ca ions play a part of acceptors. The oxygen-poor regions must yet possess properties of compensated semiconductors, as deficiency in oxygen means appearance of donors in them. Recombination of electrons belonging to un-ionized donors with holes belonging to the un-ionized acceptors is to lead to disappearance of charge carriers. Therefore the oxygen-poor regions should be characterized by a low conductivity and by an antiferromagnetic ordering.

Thus, there should be two reasons for the phase separation with respect to oxygen: (1) in the oxygen-poor region a gain in the energy should occur due to the electron-hole recombination; (2) in the oxygen-rich region a gain in the energy occurs due to establishment of the ferromagnetic ordering.

Certainly, this hypothesis has need for an experimental verification. But the aforesaid agrees with the experimental data on $La_{0.8}Ca_{0.2}MnO_{3+y}$, which is ferromagnetic at $y = 0$, but antiferromagnetic and insulating at $y = -0.2$ [72b].

Now it remains only to discuss the possibility of the irreversible inherited phase separation caused by a nonuniform impurity distribution over the crystal, i.e. by shortcomings of the sample preparation technology. But it is difficult to assume that, though almost half a century elapsed from the moment of appearance of these materials [45, 49], this technology remains so imperfect as initially, despite efforts of numerous investigators. In addition, properties of samples prepared in different laboratories using various procedures are very close to each other. For example, almost in all the samples a transition from the insulating to the metallic regime occurs at $x = 0.175$ (e.g., Refs [42, 45]). This means independence of the sample properties from its biography.

And lastly, as was established in Ref. [30], the regions of different phases differ in their conductivity more than by two orders of magnitude. Such an extremely nonuniform impurity distribution can hardly arise due to shortcomings of the technology. Rather it should be triggered by deep physical causes like those leading to the reversible phase separation.

Thus, the problem of the nature of the phase separation in the lanthanum manganites still remains to be solved experimentally.

4.4 Magnetic-field-induced insulator-metal transition in praseodymium manganites

As was described in Section 4.1, a magnetic field causes a sharp transition from the insulating state to the high-conductive state in some EuSe samples: the conductivity jump in a field of 1 T can attain 9 orders of magnitude, and the ordering in the crystal changes from antiferromagnetic to ferromagnetic. Similar phenomena are observed also in praseodymium manganites.

In Refs [73, 74], the $Pr_{0.5}Sr_{0.5}MnO_3$ compound was investigated. At low temperatures it is antiferromagnetic, and at about 140 K it displays the first-order phase transition into the ferromagnetic state (Fig. 7). In the low-temperature phase the conductivity of the sample increases with temperature as in nondegenerate semiconductors, though its value is of the same order of magnitude as in degenerate semiconductors. In the transition point the conductivity increases abruptly by the factor about 10 and further decreases with increasing temperature approaching again its low-temperature value. At temperatures below 140 K, the antiferromagnetic phase may be transformed into the ferromagnetic phase by an external magnetic field. If this field exceeds 7 T, then the crystal is ferromagnetic at any temperatures. At $T \to 0$, a field of 7 T increases the conductivity by two orders of magnitude ($\delta_H \sim -10^4\%$). Such a conductivity jump may be considered as the smallest one at which we can speak of the magnetic-field-induced insulator-to-metal transition.

A true field-induced insulator-to-metal transition was observed in $Pr_{1-x}Ca_xMnO_3$ [75 – 81]. At $x = 0.3$ several phase transitions were observed in the material [78]. At 200 K the symmetry of the crystal lattice changes, at 140 K the collinear antiferromagnetic ordering is established of so-called CE type: the ferromagnetic and antiferromagnetic atomic planes alternate, and the moments of the nearest neighbouring ferromagnetic planes are oppositely directed. Below 110 K the crystal acquires a nonsaturated spontaneous magnetization which is interpreted in Ref. [78] as a transition to a canted antiferromagnetic structure.

These conclusions were based on the analysis of neutronographic and magnetic data. The reflexes with the scattering vector $\mathbf{q} = (h, k, 0)$ correspond to the ferromagnetic long-range order, with h and k being integer and $h + k$ even. On decrease in temperature, the (1, 1, 0) peak intensity diminishes below 200 K. This was explained by the authors of Ref. [78] in terms of the formation of the Mn^{4+}-symmetry ion superlattice, which occurs simultaneously with a weak distortion of the crystal as a whole. As a consequence of this distortion, peaks appear with the indices slightly differing from integers. The intensity of the ferromagnetic peaks sharply increases below about 110 K, when the crystal acquires magnetization.

As for antiferromagnetic peaks pertaining to the CE structure, the neutron scattering vectors $\big((2n+1)/2, (2m+1)/2, 0\big)$ and $\big(n, (2m+1)/2, 0\big)$ correspond to them, where n and m are the integers. Their intensities increase sharply at 140 K and continue to grow down to lowest temperatures.

But if one assumes that the canted antiferromagnetic ordering is established over the entire crystal, then the magnitude of the magnetic moment per unit cell should be only 2.36 μ_B, whereas its expected magnitude for the Mn ions is 3.7 μ_B. In order to explain this discrepancy, it was assumed in this paper that, due to inequality of the Mn^{3+} and Mn^{4+} densities, a portion of the crystal was in the spin-glass state, i.e. the crystal was inhomogeneous.

At 4.2 K, a field of 4 T establishes the saturated ferromagnetic ordering accompanied by simultaneous crystal transition from the insulating state to the conducting one. A study of behaviour of the neutronographic spectra in the field shows that the intensity of the ferromagnetic (1, 1, 0) reflex increases with the field strength, attaining saturation at 4 T. On the contrary, the antiferromagnetic (1/2, 1/2, 0) peak disappears in this field. The (2,1; 5; 0) peaks corresponding to the distorted crystallographic structure weaken, too.

In more detail the resistivity and magnetoresistivity of the $Pr_{1-x}Ca_xMnO_3$ compounds in the range $0.3 \leqslant x \leqslant 0.5$ were investigated in Ref. [79], where it was established that the magnetic field causes the true insulator-to-metal transition.

The resistivity of all the samples studied is of the order of 10^{-2} Ohm cm at 300 K, but, on decrease in temperature, it increases by 6 – 7 orders of magnitude. A field of 6 T does not change the semiconducting character of the increase in resistivity for the sample with $x = 0.5$, when the temperature decreases down to 100 K. But in samples with $x = 0.35$ and $x = 0.3$ this field causes the transition to the high-conductive state at temperatures below 100 K. The jump in conductivity amounts to 6 orders of magnitude at $x = 0.35$, and to 4 orders of magnitude at $x = 0.3$. Both these compounds are metallic at all the temperatures in a field of 12 T. But, on decrease in temperature in this field, the $x = 0.5$ compound first decreases its resistivity, and then abruptly increases it by 3 orders of magnitude at 160 K. As a result, at lower temperatures the resistivity attains the same value as in the zero field. All these compounds display a strong hysteresis in the magnetic field. Similar results were obtained in Refs [80, 81].

One should point out some other materials with similar properties: $Nd_{0.5}Sr_{0.5}MnO_3$ [82] and compounds, which are not manganites — $La_{2-x}Sr_xNiO_3$ and $La_{1-x}Sr_xFeO_3$ [83].

The commonly accepted interpretation of the results obtained in these papers consists in the assumption of the charge ordering. This means that the insulating state of the materials under consideration is related to the hole ordering in the form of a superlattice. Namely, if the Mn^{4+} ions correspond to the holes, then these ions should alternate with the Mn^{3+} ions in a regular manner. The reason for this is the Coulomb interaction between holes which, in the case of narrow hole-energy bands, must lead to formation of some structure resembling the Wigner crystal. It looks very tempting to claim that in $Pr_{1-x}Ca_xMnO_3$ at $x = 0.5$ the Mn^{4+} and Mn^{3+} ions alternate in the 'antiferromagnetic' manner. In such a picture the transition from the insulating to the metallic state means the melting of the hole superlattice.

But this model, being undoubtedly very elegant, nevertheless simplifies the situation even in the case of materials with $x = 0.5$. First, not all the Ca and similar bivalent ions may play a part of acceptors. Strictly speaking, only those isolated from the rest of the Ca ions can be regarded as electroactive. Those of them which form clusters are not electroactive, i.e. the number of holes can be markedly lower than the number of Ca atoms. Hence, the numbers of Mn^{3+} ions and Mn^{4+} ions are not necessarily equal to each other at $x = 0.5$. Difficulties with these numbers at x less than 0.5 are still more obvious.

Furthermore, the model of the charge separation does not allow for the fact that the holes in the crystal interact with ionized acceptors via the Coulomb forces. The holes remain bound each to its acceptor up to the densities when the Mott criterion (58) of their delocalization is met. If it is not valid then the superlattice cannot exist since the very fact of its existence suggests the hole delocalization. For this reason the insulating state is not necessarily caused by the charge separation. By the way, results of neutronographic investigations [78] cited above, which give evidence to the crystallographic distortion at 200 K, cannot be univocally ascribed to the charge separation as it is done in Ref. [78].

But existence of the superlattice is not a necessary condition for the insulator-to-metal transition. It is sufficient to account for the fact that the hole effective mass decreases strongly upon transition from the antiferromagnetic state to the ferromagnetic state (cf. Eqns (60), (61)). Hence, if the Mott criterion (58) is not met in the antiferromagnetic state, it may be met in the ferromagnetic state, and then the magnetic field should cause the transition from the insulating state to the high-conductive state.

And lastly, another mechanism of this transition is a possibility. In these materials, separation into the high-conductive ferromagnetic phase and insulating antiferromagnetic phase described in Section 4.1 is possible, too. By the way, the neutronographic data [78] for the incompletely magnetized state may be interpreted not only in terms of the canted antiferromagnetic ordering but also in terms of separation into the antiferromagnetic and ferromagnetic phases. Another evidence for it is given by results [10] described in detail in Section 3.2. The phase separation makes it possible to explain the magnetic-field-induced insulator-to-metal transition here in full analogy with the explanation presented in Section 4.1 for EuSe. Hence, the phase separation theory is an alternative to the charge separation theory for these materials.

5. Resistivity and magnetoresistance of lanthanum manganites

5.1 General electric properties

As all the scenarios of the phase separation described above predict the concentration phase transition from the insulating state to the high-conductive one, we should compare this prediction with the experimental data. Really, according to Ref. [49] at x less than 0.2, the $La_{1-x}Sr_xMnO_3$ system behaves like a nondegenerate semiconductor, and from $x = 0.2$ up to $x = 0.5$ like a degenerate semiconductor with the resistivity typical of such materials, i.e. of the order of 10^{-2}–10^{-3} Ohm cm (it is several orders of magnitude lower than that for conventional metals).

Similar results were obtained in Refs [14, 42, 84] when investigating single crystals of the same system (see Fig. 8 [42]). At $x \leqslant 0.15$, the crystals are characterized by the conductivity of the semiconducting type, and at $x \geqslant 0.175$ their conductivity is of a metallic type, but close to the Curie point T_C, like in Fig. 6b, they display a conductivity peak. Thus, between $x = 0.15$ and $x = 0.175$ the percolation of the hole liquid should occur as a result of transformation of the high-conductive phase from multiply connected to simply connected. In Ref. [42], the resistivity was correlated with the crystalline structure of samples. As seen from Fig. 8, there are no marked singular features of resistivity at the points where the structural phase transition takes place.

Still earlier than in the papers just cited, the resistivity peak has been discovered on the $La_{1-x}Pb_xMnO_3$ single crystals with $0.25 < x < 0.45$ [85]. At the same temperature, which is close to the Curie point $T_C = 290$ K, the thermopower peak is located, and the magnetothermopower changes its sign. It is accepted in Ref. [85] that the low-temperature side of the resistivity peak corresponds to the metallic conductivity, and the high-temperature side does to the semiconducting conductivity with an activation energy of about 0.05 eV. A similar temperature dependence of the resistivity was observed in $La_{0.6}Pb_{0.4}MnO_{3-y}$ and $Nb_{0.6}(Sr_{0.7}Pb_{0.3})_{0.4}MnO_{3-y}$ single crystals [53]. The resistivity peak in the vicinity of the Curie point is a common feature of the ferromagnetic semiconductors [47], and its origin is explained in Sections 6.1 – 6.6 by the magnetization-dependent impurity scattering of charge carriers.

It is advisable to make here a terminological note: very often the resistivity peak in lanthanum manganites is referred

to as the metal-insulator transition. But the resistivity rise by tens or even a few hundreds of percent and its subsequent decay with the activation energy comparable to T_C, occurring with increase in temperature, cannot be treated yet as a transition from the metallic state to the semiconducting state. The true metal-semiconductor transition shows decrease in conductivity by several orders of magnitude and the activation energy greatly exceeding the thermal energy. This just the case for EuO in a certain range of the impurity density: the resistivity jump at 50 K reaches 19 orders of magnitude, and the activation energy at higher temperatures amounts to 0.3 eV (cf. Section 6.1).

An essential difference exists between results of papers [42, 53, 86] and those of other investigations on degenerate ferromagnetic semiconductors described, for example, in Ref. [47]: in the former papers the resistivity peak is found to coincide with the Curie point, whereas in the papers cited in Ref. [47] these temperatures are close to each other but do not coincide. By the way, they also do not coincide in papers [57, 87], where the $La_{1-x}Sr_xMnO_3$ single crystals were investigated, too, as well as in Refs [85, 88]. In Ref. [89] it was pointed out specially that T_C in $La_{1-x}Sr_xMnO_3$ was higher than the temperature of the resistivity peak. It should be noted that there is no coincidence of these two temperatures in manganite films as well. As an example, the $La_{1-x}Pb_xMnO_3$ films may be pointed out with T_C higher than the room temperature at x between 0.26 and 0.4 [27].

In Ref. [16], photoemission spectroscopic and X-ray absorptive studies of $La_{0.67}Ca_{0.33}MnO_3$ and $La_{0.7}Pb_{0.3}MnO_3$ made it possible to establish that above T_C a gap in the electron spectrum exists. On decrease in temperature throughout T_C, it closes, and the spectral weight at the Fermi level increases. Similar results were obtained in investigating $La_{1-x}Sr_xMnO_3$ with $x = 0.175$, i.e. close to the insulator-metal transition boundary [89]. According to spectral studies in Ref. [90a], the gap exists in the elemenary excitation spectrum of $La_{1-x}Sr_xMnO_3$ with x from 0 to 0.4. But it was recognized there that the gap was being open even in the region of the metallic conductivity, which seems strange. These spectral data correspond to a gap width of 0.2 eV at 300 K.

A very interesting problem is the way in which one might be able to determine the charge carrier density in both the uniform and phase-separated states. An attempt to carry out such measurements was made in Ref. [25], where both the longitudinal and transverse resistivity of $La_{0.67}Ca_{0.33}MnO_3$ films were measured in a perpendicular field up to 2 T. The former displayed a sharp peak in the temperature range from 230 to 270 K. This peak is shifted by the field leading to the magnetoresistance, the peak of which is located at a temperature slightly lower than the resistivity peak does.

The transverse resistivity displays a part odd in the field, and it is interpreted as the Hall resistivity. The sign of the Hall effect corresponds to holes. Their Hall concentration diminishes from 290 K down to the temperature of the resistivity peak, where it amounts to 0.01 hole per unit cell. On further decrease in temperature, the Hall concentration increases again, reaching a value of 0.3 hole per unit cell at very low temperatures. The Hall mobility is also temperature-dependent but it varies weaker than the Hall density does.

Unfortunately, it is not clear how close are these Hall quantities to their true values, because interpretation of the Hall effect in the ferromagnetic conductors is hindered by the anomalous Hall effect characteristic of them. The anomalous Hall effect may exceed the normal one by several orders of magnitude (cf. Ref. [47]). Meanwhile, the fact that according to Refs [42, 53] the resistivity of some samples is below 10^{-3} Ohm cm, i.e. it corresponds to the boundary between the resistivities of heavily doped semiconductors and amorphous metals, makes it possible to consider density values presented above as realistic.

To avoid misunderstanding, it should be noted that the hole number may differ strongly from the number of the doped bivalent atoms. This fact is well known in the physics of heavily doped semiconductors: generally speaking, not all the impurity atoms doped are electroactive. For such an atom to be electroactive, it must be separated from other impurity atoms. But, if the atom enters a complex of impurity atoms, it ceases to be electroactive. As a result, the charge carrier density can be several orders of magnitude lower than the atomic impurity density.

As the replacement of the trivalent La by bivalent atoms leads to appearance of holes in the crystal, it seems quite natural that these holes correspond to appearance of the Mn^{4+} ions instead of the Mn^{3+} ions, as just the former exist in the $CaMnO_3$ system.

But investigation of the electronic structure of $La_{1-x}Sr_xMnO_3$ at $0.2 \leqslant x \leqslant 0.6$ by the photoemission and X-ray absorption spectroscopy evidences that the holes are in the states of the oxygen type [71]. The holes are antiferromagnetically coupled with the high-spin configuration of the Mn^{3+} ion. Respectively, excitation of the electron-hole pair means the charge transfer from the oxygen p-level to the Mn d-level.

Result of Ref. [71] agrees with results of band structure calculations for the La–Ca–Mn–O system carried out by the self-consistent local-spin-density method [43]. In this paper a strong hybridization of the Mn d-levels with the oxygen p-levels is found, too.

But this is not yet the whole truth about the charge carriers in manganites. It turns out that at $x < 0.20$ the thermopower of the $La_{1-x}Sr_xMnO_3$ system changes its sign from positive to negative at temperatures higher than T_C, which means most likely that the conductivity type changes from p-type to the n-type. Moreover, in materials with $x > 0.3$ the change in the thermopower sign takes place still at the ferromagnetic ordering [90b]. A detailed explanation of this effect is absent at present, though it may be related to dispersion in energies of oxygen and Mn ions due to the randomness in impurity positions leading to several maxima and minima inside the electron (hole) band.

It is instructive to find out how strong is the influence of the hole-lattice interaction on the electric properties of manganites. As was already discussed, on change of temperature, the $La_{1-x}Sr_xMnO_3$ structure at $x = 0.15$, 0.175 and 0.2 alters from othorhombic to rhombohedral. As seen from Fig. 8, the resistivity is virtually nonsensitive to the structure phase transition. But, on the other hand, in some films the lattice distortion was found at temperatures corresponding to the resistivity peak [30].

Results of Ref. [11] point also to the possible role of the lattice thermal disordering as an origin of the resistivity. According to them, on decrease in temperature, the lattice disordering reduces much stronger that it should be in the picture of the Debye phonons. But this reduction correlates with the temperature dependence of the resistivity quite satisfactorily.

5.2 Giant negative isotropic magnetoresistance in crystals

This section will be devoted to the property most interesting for technical applications of the materials considered — their giant negative isotropic magnetoresistance (GMR) first discovered in Ref. [91]. In discussing this property one uses to take the quantity $\delta_H = \big[\rho(H) - \rho(0)\big]/\rho(H)$ as a characteristic of the relative magnetoresistance. Whereas many authors use the conventional relative magnetoresistance $\delta_0 = \big[\rho(H) - \rho(0)\big]/\rho(0)$ instead of δ_H. Under typical conditions, the quantity δ_H may exceed δ_0 by 2–3 orders of magnitude.

Typical results were obtained in investigating the $La_{1-x}Sr_xMnO_3$ system in papers [42, 84]. The main feature of the GMR consists in the fact that it is maximal at temperatures where the resistivity displays the peak at $H = 0$, i.e. close to T_C. Here it is directly related to suppression of this peak by a magnetic field. Really, all the samples display the GMR maximum in the vicinity of T_C (Fig. 9). At $x = 0.2$, when the sample remains high-conductive also at $T \to 0$, the GMR is very small at low temperatures. But in the vicinity of the concentration metal-insulator transition, GMR is considerable even at 78 K, when the crystal magnetization is close to saturated one for the phase-separated system.

Qualitatively similar results were also obtained under investigation of the same system in Ref. [14]. At $x \geqslant 0.13$ it displays the GMR cusp with a typical value of the maximal magnetoresistance $R(0)/R(10\,\mathrm{T}) = 10$. For a sample with $x = 0.1$, the GMR retains a considerable value far below the Curie point, which is close to 140 K. As this x range corresponds to the phase-separated state, where the conductivity is of nondegenerate semiconductor type, then, as was pointed out above, the large low-temperature GMR may be related to the tunnel electron transitions between ferromagnetic droplets (cf. Sections 4.1, 4.2).

But such an explanation is not likely to be universal. A significant low-temperature GMR was observed in this material also at $x = 0.25$, when the sample should possess the metallic conductivity at $T \to 0$. At low temperatures it increased with decreasing temperature, approaching to $\delta_0 = -40\%$. This value is only half the maximal value in the vicinity of T_C [58]. A similar behaviour was observed also in some films (cf. the next section). Possibly, suppression by a magnetic field of the domain structure or droplets of the insulating phase in the Fig. 6b-type phase-separated state plays an important part here.

An analysis of the temperature and field dependences of the resistivity carried out in Refs [42, 84] has led the authors to a conclusion that the resistivity depends only on the magnetization M independently of the way in which a given value of magnetization was achieved — by changes of temperature or a magnetic field. As a result, the following expression is proposed which describes GMR at relatively small magnetization values:

$$-\delta_0 = C(x)\left(\frac{M}{M_s}\right)^2,$$

where M_s is the saturation magnetization. The constant C is close to 4 in the vicinity of the metal–insulator boundary, but it decreases down to 1 at $x = 0.4$. In Ref. [31], too, in an attempt to relate specific features of the resistivity to the magnetization, a phenomenological relationship between them was deduced.

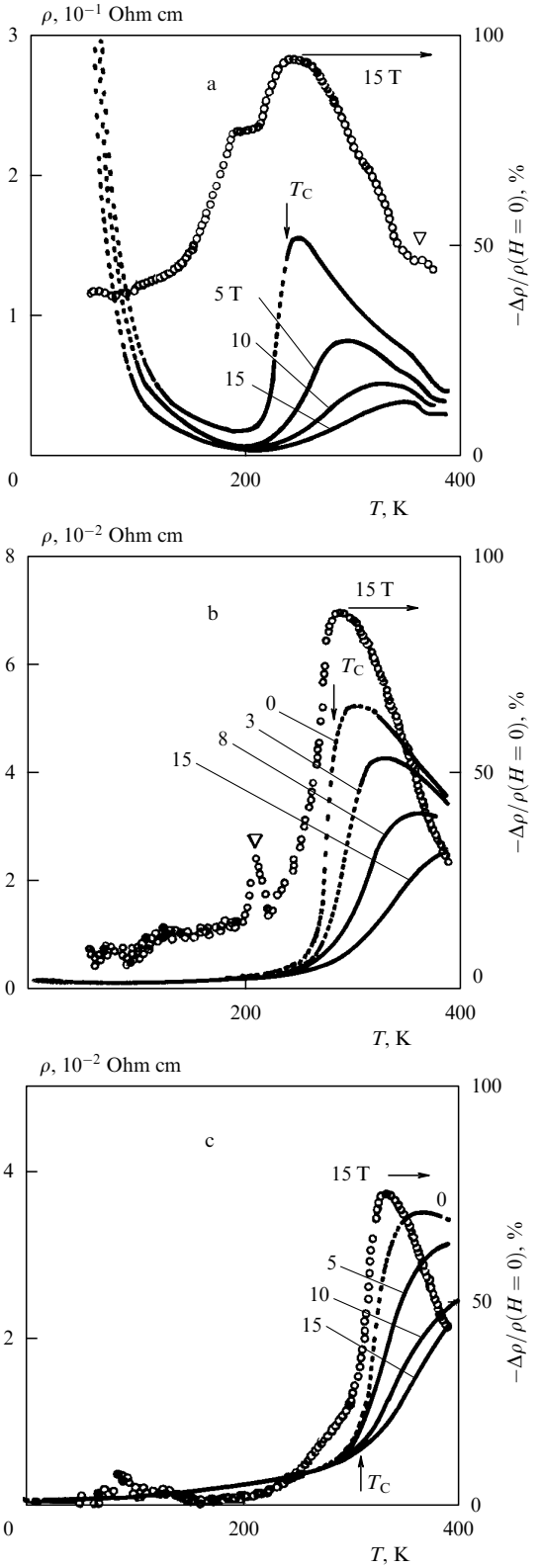

Figure 9. Temperature dependence of resistivity in $La_{1-x}Sr_xMnO_3$ crystals in various magnetic fields: (a) $x = 0.15$; (b) $x = 0.175$; (c) $x = 0.20$. The light circles correspond to $-\delta_0$-dependence in a magnetic field of 15 T; the light triangles represent the structural transitions [42].

A very large magnetoresistance was found in the $La_{1-x}Pb_xMnO_3$ single crystals: its maximal value δ_0 reaches -20% at a field strength of 1 T [85]. It was also observed in

Refs [92, 93]. In Ref. [53], the GMR was investigated in $La_{0.6}Pb_{0.4}MnO_{3-y}$ and $Nd_{0.6}(Sr_{0.7}Pb_{0.3})_{0.4}MnO_{3-y}$ single crystals. Though the qualitative similarity of these materials is obvious, an essential difference between them consists in the fact that in the former the magnetoresistance retains a large value also at room temperatures (Fig. 10).

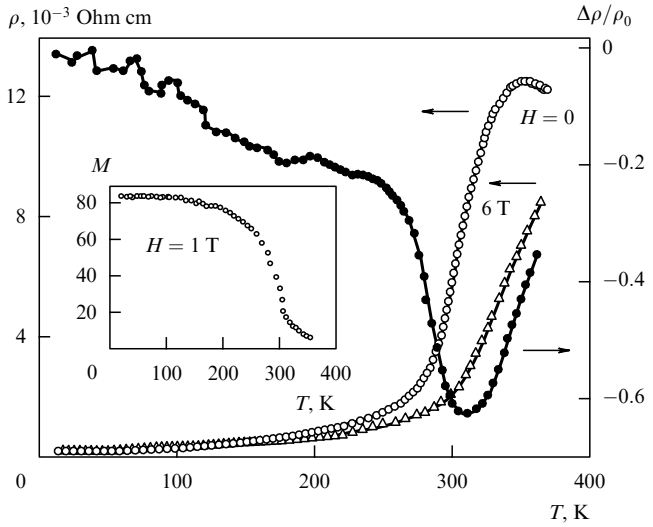

Figure 10. Temperature dependences of resistivity and magnetoresistance δ_0 for the $La_{0.6}Pb_{0.4}MnO_3$ single crystal. In the insert, the temperature dependence of the magnetization M in a 1 T field is presented for the same sample [53].

As was already mentioned in Section 4.4, the GMR was observed not only in lanthanum manganites but also in some other manganites. For example, it was found in the $Nd_{0.5}Pb_{0.5}MnO_3$ single crystals, where at 11 T the quantity δ_0 reaches -99% [94].

Both the resistivity and magnetoresistance of manganites are very pressure sensitive. The corresponding investigations were carried out on the $La_{1-x}A_xMnO_3$ system (A = Na, K, Rb, Sr) with the rhombohedral structure. Below T_C, a pressure up to 1.1 GPa reduces resistivity by more than 60%, but the effect is less pronounced above T_C. The GMR for materials under pressure amounts to $-10\%\ T^{-1}$ [95]. As was shown by studies on the $Nb_{0.5}Sr_{0.36}Pb_{0.14}MnO_{3-y}$ single crystals, the pressure reduces both the resistivity and magnetoresistance of this manganite as well [96].

Measurements on polycrystals lead, in general, to results which are close to those obtained on single crystals. For example, the $La_{1-x}Ca_xMnO_3$ polycrystals were investigated in Ref. [97]. The quantity δ_0 in them increases with decreasing temperature T_m, at which the GMR peak is located: it amounts to -90% at $T_m = 100$ K (this corresponds to $x = 0.5$), and -72% at $T_m = 240$ K ($x = 0.1$).

5.3 Giant negative isotropic magnetoresistivity in films

Investigations on manganite films are much more numerous. Their properties depend very strongly on their composition and preparation procedure. In this respect the paper [21] is very instructive. In this work the $La_{0.8}Sr_{0.2}MnO_3$ films were prepared by quite identical methods, but they were deposited on different substrates. As a result, some of them were epitaxial whereas the others were polycrystalline, and their resistivities differed by two orders of magnitude. Their temperatures of the magnetic ordering and of resistivity peaks differ very strongly, too.

On the other hand, FMR investigations on the $La_{0.67}Ba_{0.33}MnO_z$ films showed that as-deposited films are magnetically nonuniform, and they become uniform only after annealing in the oxygen atmosphere [20]. How sensitive are the properties of films to their treatment, one can see from Ref. [98], where the epitaxial films of the same composition were investigated. In the as-deposited films, the Curie temperature T_C and the saturation magnetization are essentially less than in the bulk samples. In Figs 11 and 12 the

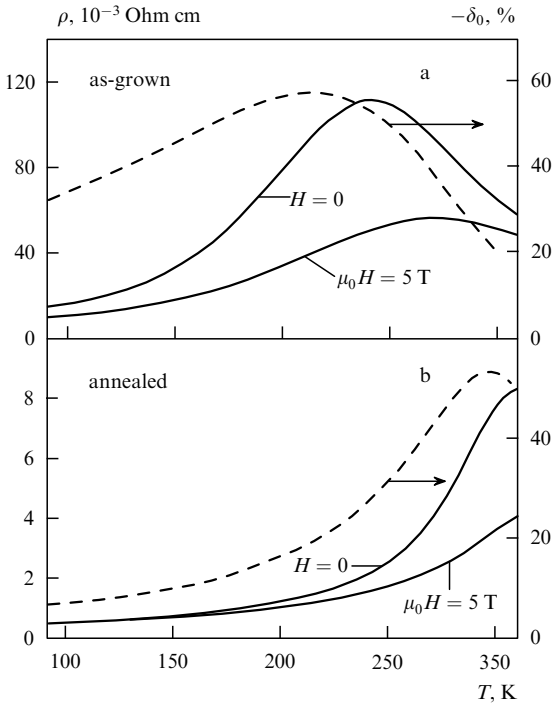

Figure 11. Temperature-dependent resistivity of the $La_{0.67}Ba_{0.33}MnO_z$ films in zero field and in a 5 T field (a) for the as-grown film deposited at 600 °C, and (b) after annealing at 900 °C for 12 hours. The dot-and-dash lines represent the magnetoresistance $-\delta_0$ [98].

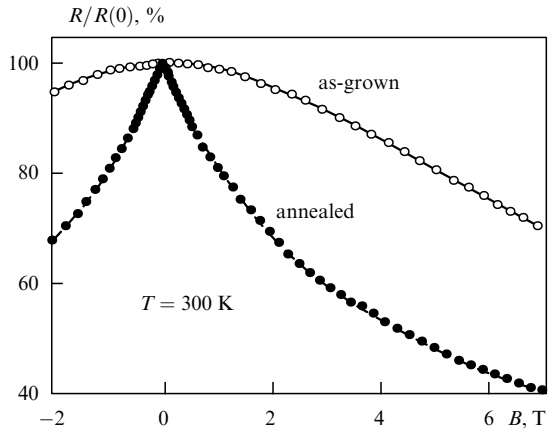

Figure 12. The resistivity vs. field (in T) at 300 K for the same samples as in Fig. 11 [98].

resistivity and magnetoresistance of these films are presented as functions of T and H. The quantity δ_0 at 300 K amounts to -60%.

In Ref. [99], the $La_{1-x}Sr_xMnO_z$ epitaxial films of a thickness about 400 nm were investigated at $0.16 \leqslant x \leqslant 0.33$. In the as-deposited films, T_C is considerably lower and the magnetic transition is much more spread than they are in the bulk samples. But annealing in the N_2 atmosphere leads to growth of their Curie points, saturation moments, conductivity and GMR as compared with the as-deposited films. For the annealed films at $x = 0.2$ and a field strength of 5 T, the relative magnetoresistance δ_0 reaches its maximum value of -60% at $T_m = 260$ K. At $x = 0.33$ the quantity δ_0 reaches its maximum value of -35% at $T_m = 330$ K. These temperatures are slightly lower than the temperatures of the resistivity peaks T_R, but they are higher than T_C determined from the maximal slope of dM/dT (M is the magnetization). For example, $T_C = 250$ K, $T_m = 260$ K, and $T_R = 290$ K at $x = 0.2$.

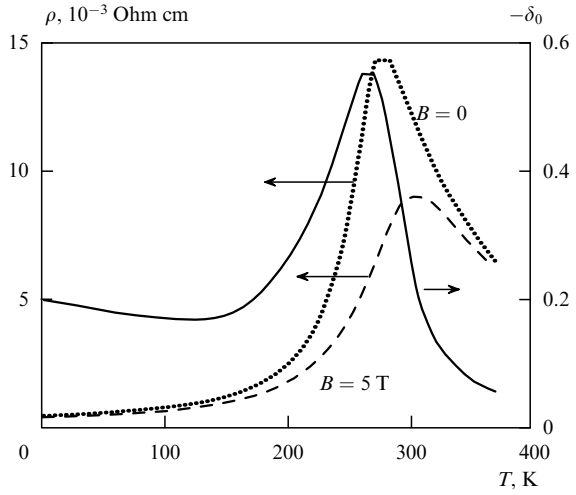

Figure 13. The temperature dependence of the resistivity and magnetoresistance ($-\delta_0$) of annealed thin $La_{1-x}Sr_xMnO_3$ films in zero field and in a 5 T field ($x = 0.16$) [99].

As seen from Fig. 13, in addition to the GMR peak in the vicinity of T_C, a low-temperature increase in GMR is observed on decrease in temperature in a film with $x = 0.16$. A similar GMR rise was observed in the $La_{1-x}Sr_xMnO_3$ single crystals (cf. the preceding section). Such an effect was also observed in some other films. For example, in the epitaxial La–Ca–Mn–O films a large magnetoresistance exists even at 5 K [8].

In the absence of the magnetic field, the resistivity of $La_{1-x}Sr_xMnO_3$ at $x = 0.16$ in the temperature range above the resistivity peak is described by the exponential temperature dependence with an activation energy of about 70 meV for the annealed films, and of about 100 meV for the as-deposited films which are close to values obtained for ceramic samples [100]. Similar expressions were proposed for a more wide class of films in [30] (but cf. Section 5.1).

The data on the $La_{0.76}Pb_{0.24}MnO_3$ films obtained by the radio-frequency sputtering and deposition on Si substrates in the mixed Ar–O_2 atmosphere, are as follows: the T_C equals 325 K, the magnetization at 4.2 K is by 14% lower than the saturation value should be. The zero-field resistivity peak is located at $T_R = 250$ K. Their GMR δ_0 is characterized by a maximal value of -22% at a field strength of 2 T, which is achived at T_R. In the whole temperature range from 4.2 to 300 K the absolute value of δ_0 remains higher than -15%, and even at 380 K it reaches 10% [27]. The $La_{0.6}Pb_{0.4}MnO_3$ films with the composition differing very little from that discussed above are characterized by $\delta_0 = -40\%$ at 300 K and a field strength of 6 T [101].

As was already pointed out above, the absolute magnetoresistance record in the manganites has been achieved in the La–Ca–Mn–O system [4]: values of δ_H amounting to $-830\,000\%$ at 125 K and to $-10^8\%$ at 57 K have been found.

Results of other authors on the same system are as follows. In Ref. [22], the magnetoresistance is investigated of the epitaxial $La_{0.67}Ca_{0.33}MnO_3$ films of a thickness 100 nm grown by the laser evaporation on the $LaAlO_3$ substrate and subjected then to a thermal treatment. Such films had a cubic structure with a lattice constant of 0.389 nm. The temperature dependence of GMR for as-deposited films is characterized by the $\delta_H(H)$ peak of a height -460% at about 100 K ($H = 6$ T). Subsequent annealing at 700 °C for 30 minutes in the oxygen atmosphere shifts the GMR peak to 200 K and increases its height up to -1400%. Further optimization processes lead to enhancement of δ_H up to $-127\,000\%$ at 77 K, which is equivalent to $\delta_0 = -93.3\%$. This is accompanied by a drop in the resistivity from 11.6 Ohm cm at zero field to 9.1 mOhm cm at $H = 6$ T. The larger portion of this drop occurs in weak fields below 6 T, which is important for practical applications.

In Ref. [102], the GMR of the $La_{0.72}Ca_{0.25}MnO_y$ films was found in still weaker fields: at $H = 1$ T and 200 K the quantity δ_0 amounted to -53%.

Here, also the zero-field resistivity peak is found, which is located at a higher temperature than the GMR peak arranged at 190 K. The GMR peak usually lies on the left side of the resistivity peak at the temperature, whereat the resistivity value is half its peak value, and where the magnetization is still significant. This result agrees qualitatively with that of Ref. [99].

The La ions in the manganite under discussion may be replaced by other trivalent rare-earth ions. An analysis of these materials leads to the conclusion [5, 103] that, on decrease in the radius of an ion replacing La, both the temperatures of the magnetic ordering and of the resistivity peak diminish, and the height of the latter increases. In stating this, one should keep in mind that the La radius exceeds the Pr radius, and the latter in turn exceeds the Y-ion radius.

In principle, nondoped materials with the La deficiency possess a high magnetoresistance, too, for example $La_{1-x}MnO_y$ ($0 \leqslant x \leqslant 0.33$). All the films deposited on the $SrTiO_3$ substrate are ferromagnetic [9, 56]. After annealing in the oxygen atmosphere, the quantity δ_H in a field of 4 T amounts to -130% at room temperature.

In some films the GMR memory effect was observed. In $Nd_{0.7}Sr_{0.3}MnO_z$ the conductivity increases linearly at initial application of the field. At temperatures essentially lower than the resistivity peak temperature T_R, the film passes to the high-conductive state ($|\delta_H| > 10^3$). This state persists even after removing the field. To return the film into the initial state, one should heat the sample up to T_R. Unlike the conductivity, the magnetization displays only a weak hysteresis [19, 104].

6. Theory of transport phenomena in degenerate ferromagnetic semiconductors

6.1 A qualitative picture of the magnetoimpurity scattering and charge carrier localization

In interpreting specific features of degenerate ferromagnetic semiconductors discussed in Sections 5.1, 5.2, the following experimental data should be considered as basic. (1) Ferromagnetic conductors with the perfect crystal lattice do not display the resistivity peak in the vicinity of T_C. Only a break in the resistivity $\rho(T)$ vs. T curve is observed at the critical point, which corresponds to the $d\rho/dT$ singularity of the same type as the heat capacity singularity. This is true both for the conductivity of the ferromagnetic metals (cf. Ref. [104]) and for the photoconductivity of semiconductors with almost perfect lattice (see Ref. [47]). (2) When the resistivity peak in the vicinity of T_C appears, it depends essentially on the impurity density. For example, in degenerate ferromagnetic semiconductors its height as a function of the donor or acceptor density passes a maximum at its certain value. This effect is most clearly pronounced in EuO, where in a narrow range of donor densities a true metal-to-insulator transition is observed with a record jump in the resistivity of 19 orders of magnitude. The insulating state preserves up to very high temperatures [105].

Almost in all the cases known the resistivity peak position does not coincide with T_C. For example, transition of degenerate EuO into the insulating state occurs at 60 K, whereas the Curie point even in the nondegenerate EuO is located at 67 K, and in a degenerate EuO it should be still higher because of the indirect exchange via conduction electrons. All this makes one search for explanation of the resistivity peak in the vicinity of T_C not in the critical charge-carrier scattering, as some authors believe, but in the interaction of charge carriers with impurity.

On the other hand, this interaction should depend on the magnetization, which is confirmed by the very existence of the resistivity peak in the vicinity of T_C, where the magnetization is strongly destroyed, and suppression of the resistivity peak by the magnetic field restoring the magnetization. The simplest version of such an interaction realizes in nondegenerate ferromagnetic semiconductors. As was earlier shown in Ref. [106], for ferromagnetic semiconductors at elevated temperatures (and still earlier in [50] for antiferromagnetic semiconductors) in the vicinity of un-ionized donor or acceptor impurities the microregions of enhanced magnetization arise which elevate the paramagnetic Curie temperature of the crystal.

In several papers an opinion was expressed that the resistivity peak in the vicinity of T_C in the ferromagnetic semiconductors of $La_{1-x}D_xMnO_3$ type is caused by charge carrier scattering by un-ionized acceptors or donors. Such an interpretation of properties of the materials under consideration is, certainly, erroneous, because un-ionized acceptors (donors) exist only in nondegenerate semiconductors, whereas the materials involved are the degenerate semiconductors, for which the notion of a separate un-ionized acceptor (donor) is meaningless. Nevertheless, it should be emphasized that the enhanced local magnetization in the vicinity of the un-ionized acceptors in nondegenerate ferromagnetic semiconductors, really, leads to the resistivity peak in the vicinity of T_C. But its origin is the temperature dependence of the charge carrier density, which passes a minimum there due to the maximal depth of the acceptor level (it is temperature-dependent, see a detailed analysis of this problem in Ref. [47]).

As for degenerate semiconductors, a main part in the nonmagnetic semiconductors plays the interaction of carriers with ionized impurities screened by other carriers. In degenerate ferromagnetic semiconductors the charge carrier scattering by fluctuations of the static magnetization should be added. These fluctuations arise due to charge-carrier-density fluctuations over the crystal, and, hence, due to fluctuations of the indirect exchange through charge carriers. In fact, though the charge carriers in degenerate ferromagnetic semiconductors are delocalized, nevertheless, their density in the vicinity of an ionized defect is higher than that far from it, since they screen its electrostatic field.

On the other hand, the charge carriers in a magnetic crystal realize the indirect exchange between the magnetic ions tending to establish the ferromagnetic ordering at not very large charge carrier densities. The higher the local charge carrier density, the stronger the local ferromagnetic exchange, and, hence, the higher is the local magnetization in a degenerate ferromagnetic semiconductor.

Obviously, the magnetization fluctuations are maximal at not-too-low and yet not-too-high temperatures. In fact, at $T = 0$ the entire crystal is magnetized maximally, and there are no magnetization fluctuations. On the contrary, at $T \to \infty$ the magnetic order is completely destroyed everywhere, and a local enhancement of the exchange interaction will not restore it. Hence, the magnetization fluctuations will be absent in this limit, too.

The effective impurity potential acting on the charge carrier is the sum of its electrostatic potential and a potential related to the local magnetization in the vicinity of the impurity. Hence, it also should be maximal at intermediate temperatures. Just there one may expect not only minimal charge carrier mobility but also the maximal degree of their Anderson localization, as a result of which the number of delocalized electrons drops. These are the origins of the resistivity peak in the vicinity of T_C. Moreover, the enhanced strength of the attractive defect can also lead to the Mott transition from the high-conductive state to the insulating state [107, 47].

At the same time, as the magnetic field suppresses the local magnetization fluctuations, it also reduces the effective impurity potential, and, hence, the charge-carrier inverse scattering time and the number in the conduction election or hole band tail below the mobility edge. This is just the mechanism for appearance of the giant isotropic negative magnetoresistance proposed in Refs [107, 47].

The mechanism corresponds to the elastic charge-carrier scattering by the static magnetization fluctuations [107, 47]. In principle, there should also exist the inelastic charge-carrier scattering by time-dependent magnetization fluctuations (i.e. magnons in the spin-wave region), which occurs together with the electrostatic scattering by impurity atoms. But this effect cannot lead to the Anderson charge-carriers localization and for this reason it is less important than the static charge-carrier scattering.

Of other theoretical papers on the subject, one may point out Ref. [12], the ideology of which is close to that presented above. In it the role is also stated of the impurity leading to the Anderson localization, and the necessity is stressed of the simultaneous accounting for the magnetic fluctuations. But the model used in Ref. [12] and the results are quite different

from those of Refs [47, 107]. It is found in the self-consistent field approximation that, on increase in temperature, of two spin subbands, the higher one becomes narrower, and the charge carriers in it may occur below the mobility edge. While in the lower band nothing of the sort happens, and for this reason the resistivity peak in the vicinity of T_C is absent. To obtain it, one should account for the ferromagnetic fluctuations mixing both the channels.

The possible role of the Anderson localization in the formation of a resistivity peak in the vicinity of T_C is discussed also in Refs [43, 108].

Along with these papers, several theoretical papers appeared, in which the role of impurities was fully ignored. For example, in Ref. [109], to explain the resistivity peak in the vicinity of T_C the Kondo lattice model with classical spins was used. In Ref. [110], based on the standard Hubbard model, an attempt was made to explain properties of the materials considered by fluctuations of charges and spins. In Ref. [6], a model Hamiltonian is proposed with a strong interaction between the charge carriers and localized spins, which ensures their normal effective mass below T_C and exponentially large one above T_C. This guarantees the metallic conductivity below T_C and the semiconducting one above T_C. But as shown in Ref. [47], in actual reality, at any coupling between the charge carriers and magnetic subsystem, the effective masses below T_C and at $T = 0$ are comparable, if not very close to each other. Apparently, the model adopted in this paper is unable to reproduce properties of real objects adequately.

Paper [32] and similar papers were criticized in Ref. [111], where it was obtained that purely exchange interactions cause peaks in the resistivity and magnetoresistivity, the height of which is as a minimum by an order of magnitude smaller than that observed in real materials. But in this paper too, the crystal lattice was treated as ideally perfect, and the attempt was made to explain their properties by an electron-phonon interaction.

It should be mentioned that the idea of the decisive role of an electron-phonon interaction is not new. Apparently, for the first time it was advanced in Ref. [38], where a detailed experimental investigation of the cooperative Jahn–Teller effect was carried out. However, this idea does not agree with the fact that the specific features of the resistivity in substituted manganites are essentially the same as in other degenerate ferromagnetic semiconductors, from which the Jahn-Teller effect is absent. In addition, as seen from Fig. 8, the change in the crystallografic structure influences the resistivity of these materials very weakly, which does not confirm the dominating role of the charge carrier–lattice interaction.

The theoretical paper [112] should be mentioned, too.

6.2 The basic Hamiltonian of the (s–d)-model

The theoretical investigation carried out below is based on the (s–d)-model, whose Hamiltonian is written in the form

$$H_{sd} = \sum E_{\mathbf{k}} a^*_{\mathbf{k}\sigma} a_{\mathbf{k}\sigma} - \frac{A}{N_t} \sum (\mathbf{S}_{\mathbf{h}} \cdot \mathbf{s})_{\sigma\sigma'} \exp\{i(\mathbf{k} - \mathbf{k}') \cdot \mathbf{g}\} \times a^*_{\mathbf{k}\sigma} a_{\mathbf{k}'\sigma'} - \frac{1}{2} \sum I(\mathbf{g} - \mathbf{f})\, \mathbf{S}_{\mathbf{g}} \cdot \mathbf{S}_{\mathbf{f}} + H_C - H \sum S^z_{\mathbf{g}}, \quad (1)$$

where $a^*_{\mathbf{k}\sigma}$, $a_{\mathbf{k}\sigma}$ are the creation and annihilation operators for the s-electron with the quasi-momentum $\mathbf{k}$ and spin projection σ, $\mathbf{S}_{\mathbf{g}}$ is the d-spin operator for atom $\mathbf{g}$, $\mathbf{s}_{\sigma\sigma'}$ are the Pauli matrices, N_t is the total number of crystal atoms over which the s-electron moves (it can also model the hole). If it moves over the magnetic atoms, index $\mathbf{h}$ in the second term of Eqn (1) coincides with $\mathbf{g}$. But, if it moves over the nonmagnetic ions (e.g., as a hole over the oxygen atoms), then $\mathbf{h}$ corresponds to the nearest magnetic neighbours of this atoms, and summation over them is carried out.

The term H_C describes the electrostatic interaction in the system of electrons and ionized donors, or in the system of holes and ionized acceptors. The last term in Eqn (1) describes the interaction of the d-spins with an external magnetic field H (in the energy units). The direct action of the field on the charge carriers is not taken into account as at not-too-low temperatures it is many orders of magnitude weaker than its indirect action through the crystal magnetization induced by the field [47].

The main parameters of the (s–d)-model constitute the s-band width $W = 2zt \propto 1/ma^2$ (m is the s-electron effective mass, a is the lattice constant under assumption of the simple cubic lattice, $\hbar = 1$); the (s–d)-exchange energy AS (S is the d-spin magnitude); the (d–d)-exchange energy zIS^2, which is of the order of temperature for the magnetic ordering in the insulating state, and the electrostatic energy $e^2 n^{1/3}/\varepsilon_0$, where n is the charge carrier density, ε_0 is the dielectric constant of the crystal, z is the coordination number.

If the hole moves over the magnetic atoms, it is in the orbital state of the d-type, and for this reason its exchange interaction with the d-electrons is very strong. On the other hand, the overlapping of the neighbouring atomic orbitals is very small. For this reason the inequality $|A|S \gg W$ should be met here. But if the hole moves over the neighbouring nonmagnetic atoms, the opposite inequality $|AS| \ll W$ should be fulfilled. In the latter case, if one is interested in the long-wave effects, then holes may be considered as moving over the cations, too. A memory for their true localization remains in a relatively small A value.

Independently of the relationship between AS and W, both these parameters should greatly exceed zIS^2, as even for narrow d-bands these quantities are of the zeroth, first and second order in the neighbouring atoms orbital overlapping, respectively.

In what follows, both the cases $AS \ll W$ and the opposite one will be discussed. At $AS \ll W$, the further inequalities will be assumed to be satisfied:

$$AS > \mu \gg \frac{e^2 n^{1/3}}{\varepsilon_0}, \quad (2)$$

where μ is the Fermi energy (below A will be taken positive). The first of inequalities (2) is a consequence of a relatively small charge carrier density in a degenerate semiconductor, the second one is the standard condition of the semiconductor degeneracy. At $AS \gg W$, the first inequality is met automatically.

6.3 The response functions to an external electric field in the case of wide s-bands

For the treatment of the static charge-carrier scattering by the magnetization fluctuations and by the electrostatic potential of the impurity atoms it is necessary to find the effective field of these defects with allowance for all the other charge carriers. First, the case of the wide bands ($AS \ll W$) will be treated, the basis for which are the results of Ref. [71] according to which the holes in manganites move over the

oxygen ions. Far from T_C the perturbation theory in AS/W is valid, so that in the first order the s-electron energy is equal to

$$E^*(\mathbf{k},\sigma) = E_\mathbf{k} - AM\sigma\,. \tag{3}$$

This equation is also valid at the magnetization M changing smoothly in the space, as in the case considered.

First of all, one should find the response functions of the system to an external electrostatic field $\Phi(\mathbf{q})$ created by ionized impurities. Naturally, it creates the external electrostatic field in a usual manner:

$$\phi(\mathbf{q}) = \varepsilon^{-1}(\mathbf{q})\,\Phi(\mathbf{q})\,, \tag{4}$$

where $\varepsilon(\mathbf{q})$ is the dielectric function of the crystal, $\mathbf{q}$ is the wave vector.

The electric field changes also the magnetization $M(\mathbf{q})$ at finite temperatures by changing the electron density. As was shown first in Refs [113, 114] for metals, in this case one may introduce the nondiagonal susceptibility relating the electric and magnetic fields. Such a magnetoelectric effect in metals where the electrons are weakly spin-polarized is rather small. But it is large in degenerate ferromagnetic semiconductors with the complete spin polarization of charge carriers. When Eqn (3) is valid, one can introduce the magnetoelectric response function ω_1 [115, 116]

$$M(\mathbf{q}) = \omega_1(\mathbf{q})\,\Phi(\mathbf{q})\,. \tag{5}$$

Hence, the effective field $\phi^*(\mathbf{q})$ acting on the electron with $\sigma = +1/2$ is given by

$$e\phi^*(\mathbf{q}) = e\phi(\mathbf{q}) - \frac{AM(\mathbf{q})}{2} \equiv e\zeta^{-1}(\mathbf{q})\,\Phi(\mathbf{q})\,, \tag{6}$$

where the 'effective dielectric function' ζ is determined as follows:

$$\zeta^{-1}(\mathbf{q}) = \varepsilon^{-1}(\mathbf{q}) - \frac{A\omega_1(\mathbf{q})}{2e}\,. \tag{7}$$

To calculate it, one should employ the condition of the constant electrochemical potential over the sample with allowance for the complete charge-carrier spin polarization (in the paramagnetic region one can achieve this with the use of a magnetic field strong enough):

$$\begin{aligned} &-\frac{AM}{2} + \mu_\mathrm{p}(n) = -\frac{AM(\mathbf{r})}{2} + e\phi(\mathbf{r}) + \mu_\mathrm{p}\bigl(n(\mathbf{r})\bigr)\,,\\ &\mu_\mathrm{p}(n) = \frac{(6\pi^2 n)^{2/3}}{2m}\,, \end{aligned} \tag{8}$$

where M and n are the values of the magnetization and charge carrier density, respectively. After linearization of Eqn (8) with respect to $\delta n(\mathbf{r}) = n(\mathbf{r}) - n$ one obtains

$$n(\mathbf{q}) = -e\phi(\mathbf{q})\,\frac{\mathrm{d}n}{\mathrm{d}\mu_\mathrm{p}}\,\frac{1}{1-\Gamma}\,, \tag{9}$$

with

$$\Gamma \cong \frac{A}{2}\,\frac{\mathrm{d}M(n)}{\mathrm{d}n}\,\frac{\mathrm{d}n}{\mathrm{d}\mu_\mathrm{p}}\,. \tag{10}$$

In calculating the dielectric function of the crystal one should keep in mind that the electrostatic field acting in the crystal is the sum of the external field $\Phi(\mathbf{q})$ reduced by a factor of ε_0 due to the crystal polarization, and the field $\delta\phi(\mathbf{q})$ produced by the charge carriers:

$$\delta\phi(\mathbf{q}) = \phi(\mathbf{q}) - \frac{\Phi}{\varepsilon_0} = \left[1 - \frac{\varepsilon(\mathbf{q})}{\varepsilon_0}\right]\phi(\mathbf{q})\,. \tag{11}$$

Use of Eqn (9) makes it possible to represent the Poisson equation for the electron part of the electrostatic field in the form

$$q^2\delta\phi(\mathbf{q}) = -4\pi e^2\,\frac{\mathrm{d}n}{\mathrm{d}\mu_\mathrm{p}}\,\frac{\phi(\mathbf{q})}{\varepsilon_0(1-\Gamma)}\,. \tag{12}$$

Then from Eqns (11), (12) one may deduce the following expression for the dielectric function of the conducting magnetic crystal:

$$\begin{aligned} &\varepsilon(\mathbf{q}) = \varepsilon_0 + \frac{\varkappa^2}{q^2}\,,\\ &\varkappa^2 = \frac{\varkappa_\mathrm{p}^2}{1-\Gamma}\,,\quad \varkappa_\mathrm{p}^2 = 4\pi e^2\,\frac{\mathrm{d}n}{\mathrm{d}\mu_\mathrm{p}}\,. \end{aligned} \tag{13}$$

In the long-wave approximation used here the magnetoelectric response function $\omega_1(\mathbf{q})$ is easily found from Eqns (5), (8), (9):

$$\omega_1(\mathbf{q}) = -\frac{2e\Gamma}{A(1-\Gamma)\,\varepsilon(\mathbf{q})}\,. \tag{14}$$

In writing Eqn (14) the derivative $\mathrm{d}M(\mathbf{q})/\mathrm{d}n(\mathbf{q})$ was replaced by $\mathrm{d}M/\mathrm{d}n$ since its $\mathbf{q}$-dependence is much weaker than that of $\varepsilon(\mathbf{q})$.

With allowance made for Eqns (13), (14) the effective dielectric function (7) is found to be

$$\zeta(\mathbf{q}) = \varepsilon(\mathbf{q})\,(1-\Gamma) = \varepsilon_0(1-\Gamma) + \frac{\varkappa_\mathrm{p}^2}{q^2}\,. \tag{15}$$

As seen from this equation, the effective dielectric function $\zeta(\mathbf{q})$ differs from the true one $\varepsilon(\mathbf{q})$ in replacement of the true dielectric constant ε_0 by the effective dielectric constant

$$\zeta_0 = \varepsilon_0(1-\Gamma)\,. \tag{15a}$$

According to (10), in order to determine Γ and, hence, ζ_0, it suffices to establish the M dependence on n.

In the paramagnetic region, with allowance made for the complete spin polarization of charge carriers in the magnetic field and Eqn (3), the self-consistent field equation is written as follows:

$$M = SB_S\left[\left(H + zIM + \frac{Anv}{2}\right)\frac{S}{T}\right], \tag{16}$$

where $B_S(x)$ is the Brillouin function, $v = a^3$. One obtains from Eqns (10), (16):

$$\begin{aligned} &\Gamma = \frac{3}{8}\,\frac{A^2 nvSB_S'}{\mu_\mathrm{p}(T - zISB_S')}\,,\\ &B_S' = \frac{\mathrm{d}B_S(x)}{\mathrm{d}x}\,,\quad x = \left(H + zIM + A\,\frac{nv}{2}\right)\frac{S}{T}\,. \end{aligned} \tag{17}$$

In the spin-wave region, if the inequalities $T_C/S \ll T \ll T_C$ are met, one may write

$$M = S - \frac{T}{N}\sum_{\mathbf{q}} \frac{1}{\Omega_{\mathbf{q}}}\,, \tag{18}$$

where $\Omega_{\mathbf{q}}$ is the frequency of the ferromagnetic magnon, N is the number of magnetic atoms. To specify Eqn (18), one should take into account that the ferromagnetic ordering in a crystal is determined by the direct and indirect exchange interactions simultaneously. The latter cannot be described by the standard RKKY theory, as the applicability condition of the RKKY theory, $\mu \gg AS$, is opposite to the condition (2). The corresponding calculations performed in Refs [117, 118] are presented in [47]:

$$\Omega_{\mathbf{q}} = H + J(1-\gamma_{\mathbf{q}}) + \frac{Anvq^2}{2(q^2+q_0^2)}\,, \tag{19}$$

where the following notations are used:

$$J = zIS, \qquad q_0^2 = 2mAS\,. \tag{20}$$

Consequently, in this case the quantity Γ is given by the expression

$$\Gamma = \frac{A^2Ta^3}{4}\,\frac{\mathrm{d}n}{\mathrm{d}\mu}\,\frac{1}{N}\sum\frac{q^2}{\Omega_{\mathbf{q}}^2(q^2+q_0^2)}\,. \tag{21}$$

It should be noted that use of the fluctuation-dissipation theorem and a graphical technique for the temperature Green's functions made it possible to calculate the response functions for any wave vectors $\mathbf{q}$. In particular, a rather complicated expression for the quantity $\Gamma(\mathbf{q})$ was found, which goes to the quantity Γ (21) at $\mathbf{q}=0$ [115, 116, 119a, 47]. The long-wave limit at an arbitrary spin polarization was investigated in [119b].

6.4 The response functions in the critical region

The situation is still more complicated in the vicinity of T_C. Equation (3) suggests that the electron energy depends on the long-range order and, hence, its spin projection is a conserved quantity. Meanwhile, it follows from simple physical argumentation that the electron energy can depend only on the short-range order. Applicability of Eqn (3) is simply a consequence of the fact that at certain temperatures the long-rang order and short-range order virtually coincide.

One may persuade oneself in the decisive role of the short-range order by the analysis of the well-known expression for the s-electron energy in the system of the spiral ordered classical d-spins ($\mathbf{Q}$ is the wave vector of the structure) [120, 121]:

$$E(\mathbf{k},\pm) = \frac{1}{2}\left\{E_{\mathbf{k}} + E_{\mathbf{k}+\mathbf{Q}} \pm \left[(E_{\mathbf{k}} - E_{\mathbf{k}+\mathbf{Q}})^2 + A^2S^2\right]^{1/2}\right\}. \tag{22}$$

It follows from Eqns (22), (20) and (3) that at $Q \ll q_0$ the minimal electron energy is virtually equal to $(-AS/2)$, i.e. it is the same as for a ferromagnet, though the average magnetization of the interior of the spiral structure is zero. On the other hand, in the interior of the spiral structure, the short-range ferromagnetic order retains over a length small compared to the spiral period $\sim Q^{-1}$. In physical terms this means that the electron energy is not determined by the long-range order but by the short-range order over a length of $\sim q_0^{-1}$.

If the local moment direction changes smoothly (large Q^{-1}), spin of an electron close to the conduction band bottom adjusts to the direction of the local moment ensuring practically the full gain in the (s–d)-exchange energy. Mathematically, this means the nonanalyticity of the electron energy in AS/W at small Q. But at large Q the electron energy is analytical in this parameter, as the electron spin is not able to adjust to rapid change in the direction of the local magnetic moment .

Close to T_C the long-range order is practically absent, but the short-range order is still very essential, and the local magnetization changes smoothly over the crystal. For this reason in the vicinity of T_C the gain should be also considerable in the electron energy due to the short-range order. Like the case of the spiral ordering, to realize it, the s-electron spin should not be a conserved quantity, but ought to adjust to the local moment direction.

A variational procedure for calculating the electron states directly at T_C was developed in Refs [122], [123] and later generalized for the vicinity of T_C, and its validity was proved by comparison with results of calculation for the electron states in the spin-wave region obtained in the first order in $1/S$. It reproduces not only Eqn (3) but even a result valid at $T \ll T_C/S$ [107]. The latter is especially important, as long-wave magnons dominate in this temperature range and, hence, like in the vicinity of T_C, the local magnetization changes smoothly over the crystal. In addition, results of Refs [122, 123] are confirmed by the direct summation of an infinite sequence of the perturbation (in AS/W) theory graphs carried out with the accuracy of a numerical factor in Ref. [124].

The procedure may be established as follows. It is assumed that when the s-electron is on the atom $\mathbf{g}$, its spin is aligned with the local moment, the role of which is played by the moment $\mathbf{M}_{\mathbf{g}}$ of the spherical region $G_{\mathbf{g}}$ of radius R centred at this atom. At finite R the mean magnetization $M_{\mathbf{g}}(R)$ of the $G_{\mathbf{g}}$ region per atom is nonzero, diminishing with increasing R. For this reason the gain in the (s–d)-exchange energy (the second term in Eqn (1)) reduces with increasing R .

On the other hand, the directions of the moments of the first neighbouring atoms $\mathbf{M}_{\mathbf{g}}$ and $\mathbf{M}_{\mathbf{g}+\boldsymbol{\Delta}}$ differ from each other. For this reason after going over from the one of these atoms to the other, the s-electron spin turns by the angle $\theta_{\mathbf{g},\,\mathbf{g}+\boldsymbol{\Delta}}$ between these moments. At small $\theta_{\mathbf{g},\,\mathbf{g}+\boldsymbol{\Delta}}$ it leads to the replacement of the hopping integral t, to which the first term in Eqn (1) is proportional in the first nearest neighbour approximation, by the effective hopping integral

$$t_{\mathrm{eff}}\,(\mathbf{g},\mathbf{g}+\boldsymbol{\Delta}) = t\cos\frac{\theta_{\mathbf{g},\,\mathbf{g}+\boldsymbol{\Delta}}}{2}\,. \tag{23}$$

Obviously, the larger the angle $\theta_{\mathbf{g},\,\mathbf{g}+\boldsymbol{\Delta}}$, the higher the s-electron band bottom. As this angle increases with diminishing size of the G regions, then, contrary to the (s–d)-exchange energy, the electron kinetic energy enhances. The optimal radius R should be found from the condition of the minimal electron energy at the band bottom.

In carrying out the calculation, the electron trial function is chosen in the form of a plane wave with the spin direction fluctuating together with the local magnetic moment fluctuations. After thermodynamic averaging of an expression for the s-electron energy over d-spins, it turns out to be expressed

in terms of the spin correlation functions:

$$E^{\mathrm{F}}_{\mathbf{k}\lambda} = -\frac{W}{2}\left(1-\frac{P}{4}\right)\gamma_{\mathbf{k}} - A\lambda Q\,, \tag{24}$$

$$1-\frac{P}{4} \simeq \cos\frac{\theta_{\mathbf{g},\,\mathbf{g}+\mathbf{\Delta}}}{2}\,, \quad P = 1-\left\langle\frac{|\mathbf{M}_0\cdot\mathbf{M}_{\mathbf{\Delta}}|}{|\mathbf{M}_0||\mathbf{M}_{\mathbf{\Delta}}|}\right\rangle,$$

$$Q = \left\langle\frac{\mathbf{S}_0\cdot\mathbf{M}_0}{|\mathbf{M}_0|}\right\rangle, \quad \gamma_{\mathbf{k}} = \frac{1}{z}\sum_{\mathbf{\Delta}}\exp(\mathrm{i}\mathbf{k}\cdot\mathbf{\Delta})\,,$$

where the angular brackets denote the thermodynamic averaging, λ is the electron spin projection onto the local moment direction, $W = 2zt$. After replacement of $|\mathbf{M}_{\mathbf{g}}|$ by $\langle\mathbf{M}^2_{\mathbf{g}}\rangle^{1/2}$, the composite spin correlation functions in Eqn (24) get expressed in terms of the binary spin correlation functions. For the latter the expressions of the Ornstein–Zernike type are used:

$$\langle S^z_0 S^z_{\mathbf{f}}\rangle = M^2 + rS(S+1)\,\frac{\exp(-\xi f)}{f}\,, \tag{25}$$

$$\langle S^x_0 S^x_{\mathbf{f}}\rangle = \langle S^y_0 S^y_{\mathbf{f}}\rangle = \frac{rS(S+1)}{f}\,, \quad f = |\mathbf{f}|\,. \tag{26}$$

The latter circumstance makes it possible to represent the inverse correlation length ξ below T_{C} as a quantity proportional to the average magnetization M^2, since they both are proportional to $T_{\mathrm{C}} - T$ in this approximation:

$$M = c\tau^{1/2}, \qquad \xi = b\,|\tau|\,,$$

$$\tau = 1-\frac{T}{T_{\mathrm{C}}}, \qquad c\sim S, \qquad \frac{1}{b}\sim r\sim a\,, \tag{27}$$

$$\xi = gM^2, \qquad g = \frac{b}{c^2}\sim\frac{1}{aS^2}\,. \tag{28}$$

The spin correlation functions in Eqn (24) are calculated by replacement of the summation by integration, and then the expression obtained is minimized with respect to R:

$$E^{\mathrm{F}}_{\mathbf{k},1/2} = E^{(0)}_{\mathbf{k}} + E^{(2)}_{\mathbf{k}} M^2\,, \tag{29}$$

$$E^{(0)}_{\mathbf{k}} = -\frac{3A}{4}\left(\frac{5l}{6R_0}\right)^{1/2}\left(1+\frac{\gamma_{\mathbf{k}}}{4}\right) - \frac{W\gamma_{\mathbf{k}}}{2}\,, \tag{30}$$

$$E^{(2)}_{\mathbf{k}} = -\frac{11A}{48}\left(\frac{5R_0}{6l}\right)^{1/2}\left(1+\frac{\gamma_{\mathbf{k}}}{4}\right)p\,, \tag{31}$$

$$p = 1-gS(S+1), \qquad l = 3rS(S+1)\,. \tag{32}$$

The optimal radius of the short-range-order region is given by the formula

$$R = R_0\left(1-\frac{pR_0M^2}{9l}\right), \tag{33}$$

$$R_0 = \left(\frac{Wa^2}{3A}\right)^{2/3}\left(\frac{5}{6l}\right)^{1/3} \gg a\,. \tag{34}$$

As is followed from Eqns (29) – (34), in the vicinity of T_{C} the shift of conduction band bottom in a ferromagnetic crystal as compared with a nonmagnetic crystal is of the order of

$$AS\left(\frac{a}{R_0}\right)^{1/2} \sim AS\left(\frac{AS}{W}\right)^{1/3}.$$

Under real conditions at $AS/W \ll 1$, the quantity $(AS/W)^{1/3}$ may be of order unity, i.e. this shift may be comparable with the shift at $T = 0$ which is as high as $AS/2$.

Furthermore, unlike Eqn (3), the conduction band bottom is not linear but quadratic in magnetization. This is a consequence of the fact that the electron energy in the vicinity of T_{C} is determined mainly by the short-range order, and the long-range order is an analogue of an external magnetic field, in the strength of which the electron energy may be only quadratic as there is no other fixed vector in the system.

The response functions will be considered hereinafter under assumption that s-electrons occupy only states with the spin projection $\lambda = 1/2$ onto the direction of the local moment. As the electron energy depends on the magnetization M quadratically, the magnetoelectric response function is introduced here in the following manner:

$$M^2(\mathbf{q}) = \omega_2(\mathbf{q})\,\Phi(\mathbf{q})\,. \tag{35}$$

Then with allowance made for Eqns (4) and (29) one finds the expression for the effective dielectric function :

$$\frac{1}{\zeta(\mathbf{q})} = \frac{1}{\varepsilon(\mathbf{q})} + E^{(2)}_{\mathbf{q}}\omega_2(\mathbf{q})\,, \tag{36}$$

which is valid at $q \ll \min\{R_0^{-1},\, n^{-1/3}\}$.

The condition of the constant electrochemical potential takes the form (cf. (8)):

$$\mu_{\mathrm{p}}\big(n(\mathbf{r})\big) = \mu_{\mathrm{p}}(n) - e\phi(\mathbf{r}) - E^{(2)}_0\big[M^2(\mathbf{r}) - M^2\big]\,. \tag{37}$$

Putting $\delta M^2(\mathbf{r}) = M^2(\mathbf{r}) - M^2$, $\delta n(\mathbf{r}) = n(\mathbf{r}) - n$ and linearizing Eqn (37), one again arrives at Eqn (9), but with account for Eqns (27) – (29) the quantity Γ is given here at $H = 0$ by

$$\Gamma = -E^{(2)}_0\,\frac{\partial M^2}{\partial T_{\mathrm{C}}}\,\frac{\mathrm{d}T_{\mathrm{C}}}{\mathrm{d}n}\,\frac{\mathrm{d}n}{\mathrm{d}\mu_{\mathrm{p}}}\,. \tag{38}$$

From Eqns (9), (38) using the previous argumentation, one obtains the following expression for ω_2:

$$\omega_2(\mathbf{q}) = e\,\frac{\mathrm{d}M^2}{\mathrm{d}n}\,\frac{1}{(1-\Gamma)\,\varepsilon(\mathbf{q})}\,. \tag{39}$$

In the long-wave limit, after replacement of $E^{(2)}_{\mathbf{q}}$ by $E^{(2)}_0$ in Eqn (36), one finds the expression for the effective dielectric function $\zeta(\mathbf{q})$ coinciding with Eqn (15), but the quantity Γ is given here by Eqn (38).

At this stage, the problem is reduced to determination of the T_{C} dependence on n under conditions of a non-RKKY indirect exchange. If this exchange is much weaker than the direct ferromagnetic exchange, one may find the electron-induced shift δT_{C} of the Curie point with the aid of the theorem on small additions to a thermodynamic potential [125]. It follows from Eqn (24) for the free energy F:

$$F = 3N(T-T^0_{\mathrm{C}})\,\frac{M^2}{2S(S+1)} + nE^{(2)}_0M^2 + O(M^4, n^{5/3}M^2)\,. \tag{40}$$

Here the first term corresponds to the undoped ferromagnet with the Curie point T^0_{C}. Then one obtains from Eqn (40):

$$\delta T_{\mathrm{C}} = -\frac{2}{3}\,E^{(2)}_0 S(S+1)\,nv\,. \tag{41}$$

In a general case we can evaluate T_{C} more crudely by extrapolating Eqns (18), (19) to T_{C}, i.e. putting $M = 0$ in

them:

$$\delta T_C \sim (ASW)^{1/2} nv \tag{42}$$

at a weak indirect exchange (this result is close to Eqn (41)), and

$$T_C = \frac{ASnv}{2} \tag{43}$$

for the dominating indirect exchange.

As is followed from Eqns (27) – (29), (38), (41), (43), when the indirect exchange is weak, then

$$\Gamma = (E_0^{(2)})^2 S(S+1)\, \frac{b}{gT_C\mu_p}\, nv\,. \tag{44}$$

In the opposite limiting case, when it dominates, we get

$$\Gamma = \frac{3}{2}\left|E_0^{(2)}\right| \frac{b}{g}\, \frac{1}{\mu_p}\,. \tag{45}$$

6.5 The response functions at the double exchange

Now the case $W \ll AS$ corresponding to the double exchange will be considered at temperatures when the spin-wave approximation is valid. In this case the (s–d)-exchange is taken into account in the zeroth order, and for this reason its energy $(-AS/2)$ does not depend on d-spin directions with respect to each other. But the effective hopping integral depends on them. Such a situation was investigated for the first time in Refs [126, 127] for the case of two d-spins between which a single electron is going back and forth. Since then it is referred to as the double exchange.

The case of an arbitrary large number N of d-spins was investigated in Ref. [62], where the effective Hamiltonian of the double exchange was constructed. As compared with the initial Hamiltonian (1), the number of parameters entering it is smaller by unity, as the (s–d)-exchange energy $(-AS/2)$ is excluded from it. In this respect it resembles the Hamiltonian of the t–J-model, from which the constant is also excluded which corresponds to the on-site interaction. But unlike the latter, the double exchange Hamiltonian is valid for any d-spin magnitude.

As the structure of the double exchange Hamiltonian is very complicated, its simplified deduction will be presented below, which is valid for the spin-wave region [47]. In the zeroth approximation, spins of the s-electron and of an atom at which it is located, form a combined spin of magnitude $S + 1/2$ (at $A > 0$). Thus, if there is only one s-electron in the system, then one atom in the crystal has the spin of magnitude $S + 1/2$, and the rest of atoms have the spins of magnitude S. In the ferromagnetic state all the spins, independently of their magnitude, are aligned 'up'.

In the first approximation in W/AS, the electron may go over between atoms. Respectively, the 'irregular' spin changes its position. But the total moment of the crystal remains maximal, i.e. equal to $NS + 1/2$. In fact, such a state corresponds to a uniform mixed-valence state as the average spin of each atom lies between S and $S + 1/2$.

The magnon signifies a spin deflection from the total moment direction, which moves over all the atoms of the crystal independently of their spin magnitude. For this reason for atom $\mathbf{f}$ one may introduce operators $b_\mathbf{f}^*$, $b_\mathbf{f}$ of the deflection of its spin from its maximal projection value, which do not depend on its magnitude. Evidently, at a fixed value of the total moment, the total magnon number should be a conserved quantity.

In a similar manner one may introduce operators of the spinless fermions $a_\mathbf{f}^*$, $a_\mathbf{f}$ corresponding to location of an s-electron on atom $\mathbf{f}$ in the state when its spin is combined with the spin of this atom to form a total spin. If one takes the initial electron Hamiltonian (1) in the nearest neighbour approximation in an attempt to construct the corresponding effective Hamiltonian by its expansion in the magnon operators, it must have the structure conserving the total magnon number:

$$H_{\rm eff} = H_0 + H_2 + O(b^* b^* bb)\,, \tag{46}$$

$$H_0 = -t \sum a_\mathbf{g}^* a_{\mathbf{g}+\mathbf{\Delta}}\,,$$

$$H_2 = -t \sum \left\{ X(b_\mathbf{g}^* b_\mathbf{g} + b_{\mathbf{g}+\mathbf{\Delta}}^* b_{\mathbf{g}+\mathbf{\Delta}}) + Y b_\mathbf{g}^* b_{\mathbf{g}+\mathbf{\Delta}} + Z b_{\mathbf{g}+\mathbf{\Delta}}^* b_\mathbf{g} \right\} a_\mathbf{g}^* a_{\mathbf{g}+\mathbf{\Delta}}\,.$$

To find the unknown coefficients X, Y and Z, the single-electron single-magnon wave function is represented as an expansion in the functions $a_\mathbf{g}^* b_\mathbf{h}^* |0\rangle$, where $|0\rangle$ is the vacuum wave function, and the expansion coefficients are compared with expansion coefficients for the eigenfunctions of the (s–d)-exchange Hamiltonian (the second term in (1)) corresponding to the same spin projection. As a result, in the first order in $1/S$ one arrives at the desired relationship with allowance made for the direct exchange:

$$H_{\rm eff} = -zt \sum \gamma_\mathbf{k} a_\mathbf{k}^* a_\mathbf{k} - \frac{zt}{4SN} {\sum}' (\gamma_\mathbf{k} + \gamma_{\mathbf{k}'} - 2\gamma_{\mathbf{k}+\mathbf{q}}) \times b_\mathbf{q}^* b_{\mathbf{q}'} a_\mathbf{k}^* a_{\mathbf{k}'} + \sum \left[H + J(1-\gamma_\mathbf{q})\right] b_\mathbf{q}^* b_\mathbf{q}\,. \tag{47}$$

The prime over the sum in the second term in Eqn (47) enforces a the law of the total quasi-momentum conservation.

One obtains from Eqn (47) the following expression for the renormalized electron energy:

$$E_\mathbf{k} = -zB\gamma_\mathbf{k}\,, \tag{48}$$

$$B = t\left[1 - \frac{1}{2SN} \sum (1-\gamma_\mathbf{q}) f_\mathbf{q}\right],$$

where $f_\mathbf{q} = f(\Omega_\mathbf{q}/T)$ is the magnon distribution function. With allowance made for Eqn (47), the renormalized magnon frequencies $\Omega_\mathbf{q}$ can be written at small number v of the charge carriers per atom as follows:

$$\Omega_\mathbf{q} = H + \left[J + zt\,\frac{\lambda}{2S}\right](1-\gamma_\mathbf{q})\,, \tag{49}$$

$$\lambda = \frac{1}{N} n_\mathbf{k} \gamma_\mathbf{k} \simeq nv \equiv v\,,$$

where $n_\mathbf{k}$ is the Fermi distribution function.

According to Eqns (48), (49) in the case under consideration, the electron effect on the magnetization manifests itself through dependence of their band width on their density. Respectively, one should introduce an indirect magneto-electric response function which relates the local conduction-band-bottom position $C = -zB$ to the electric field [128]:

$$C(\mathbf{q}) = \beta(\mathbf{q})\, \Phi(\mathbf{q})\,. \tag{50}$$

Strictly speaking, the renormalization of the hopping integral ought to lead also to the renormalization of the s-electron effective mass $m = (2Ba^2)^{-1}$, i.e. the electric field Φ affects the effective mass as well. But one may neglect this as the effective-mass field dependence manifests itself only in the electron kinetic energy, which is of the order of $Wv^{2/3}$, i.e. it is small as compared to W at small v. Hence, the effective field $\phi^*(\mathbf{q})$ acting on the electron is

$$e\phi^*(\mathbf{q}) = e\phi(\mathbf{q}) + C(\mathbf{q}) \equiv e\,\zeta^{-1}(\mathbf{q})\,\Phi(\mathbf{q}) \tag{51}$$

with the effective dielectric function

$$\zeta^{-1}(\mathbf{q}) = \varepsilon^{-1}(\mathbf{q}) + \frac{\beta(\mathbf{q})}{e}\,. \tag{52}$$

Using, as before, the condition of constant electrochemical potential, one obtains the following expression for the quantity Γ entering Eqn (9):

$$\Gamma \cong -\frac{\mathrm{d}C}{\mathrm{d}n}\,\frac{\mathrm{d}n}{\mathrm{d}\mu}\,. \tag{53}$$

For the effective dielectric function Eqn (15) remains in force. Using Eqns (48), (49) and (100), one obtains for Γ:

$$\Gamma = -\frac{3}{2}\,\frac{1}{(6\pi^2)^{2/3}}\left(\frac{zt}{2S}\right)^2\frac{1}{B}\,\frac{1}{N}\sum(1-\gamma_{\mathbf{q}})\,\frac{\mathrm{d}f_{\mathbf{q}}}{\mathrm{d}\Omega_{\mathbf{q}}}\,. \tag{54}$$

At $T_C \gg T \gg T_C/S$ and $H = 0$, putting $z = 6$ one finds from (54)

$$\Gamma = \frac{48}{(6\pi^2)^{2/3}}\,\frac{tTv^{1/3}}{(2SJ + 6tv)^2}\,. \tag{55}$$

6.6 The resistivity peak, metal–insulator transition and giant magnetoresistance

The results presented in this section make it possible to explain adequately the specific features of degenerate ferromagnetic semiconductors. There are two mechanisms by which the magnetoimpurity interaction affects their resistivity: the charge-carrier scattering reducing their mobility, and formation of the band tail consisting of localized states. Hence, due to the band tail, the number of delocalized charge carriers diminishes.

To describe the charge-carrier scattering by randomly distributed ionized impurities in a magnetic crystal, one should replace the true dielectric function $\varepsilon(\mathbf{q})$ by the effective dielectric function $\zeta(\mathbf{q})$ (15) in the expression for their effective potential. According to Eqns (15), (15a) this means replacement of the true dielectric constant ε_0 by the effective dielectric constant $\zeta_0 = \varepsilon_0(1-\Gamma)$. Then the following modified Brooks–Herring expression is obtained for the relaxation time τ_k [47]:

$$\tau_k^{-1} = 2\pi\,\frac{e^2nm}{k^2\zeta_0^2}\left[\ln(1+\eta) - \frac{\eta}{1+\eta}\right],\quad \eta = \frac{4k^2\zeta_0}{\varkappa^2}\,. \tag{56}$$

As for the density-of-states tail inside the forbidden gap, with increase in the distance E_c from the bottom of the electron or hole band, the density of states in the tail diminishes according to the exponential law, which is nothing more nor less than generalization of the well-known law for nonmagnetic semiconductors (cf. [47]):

$$g(E) \propto \exp\left\{-\frac{(E-E_c)^2}{E_f^2}\right\}, \tag{57}$$

$$E_f \propto \frac{e^2n^{1/3}}{\zeta_0}\left(\frac{\zeta_0}{n^{1/3}me^2}\right)^{1/12}.$$

Thus, the total number of charge carriers in the localized tail states is proportional to E_f.

Strictly speaking, in Eqns (56), (57) one may use expressions for ζ_0 calculated at the fixed total charge-carrier density n only when the number of charge carriers in the tail is small compared to the number of delocalized charge carriers. But one should keep in mind that, in actual reality, the effective impurity potential is determined not only by completely delocalized charge carriers but also localized charge carriers, the localization length of which being comparable to the screening length. For this reason Eqns (56), (57) may be valid even at a considerable number of localized charge carriers.

As seen from Eqns (15a), (56), (57), decrease in ζ_0 leads to enhancement in both the charge carrier scattering and its number in localized states. As the total carrier number is fixed, this signifies the reduction in the number of delocalized charge carriers, which should be still more important effect than the reduction in their mobility does. Hence, in order to establish the specific features of the resistivity and magnetoresistance, it is sufficient to analyze the Γ-dependences on temperature and magnetic field.

Let us first discuss the case of wide s-bands. As is followed from Eqn (21), at a fixed field H in the spin-wave region the quantity Γ increases with temperature. But according to Eqn (17) in the paramagnetic region Γ decreases on increase in T. Strictly speaking, Eqn (17) is obtained only for sufficiently strong fields when all the charge carriers are spin-polarized. But if this condition is not met, then the magnetoelectric effect should be considerably less pronounced, and then one may approximately put $\Gamma = 0$. Consequently, Γ ought to be maximal at temperatures of order T_C, though its maximum does not coincide generally with T_C. Respectively, the resistivity peak position does not coincide with T_C.

Moreover, it may turn out that in this temperature range the transition from the high-conductive state to the insulating one takes place. This means that all the charge carriers get localized in the band tails, i.e. the Fermi level is below the mobility edge.

If the direct exchange is ferromagnetic, then, as seen from Eqns (44), (45), at relatively small n the quantity Γ increases with n. But, on further increase in n, it should pass the maximum at a certain density $n_{\max}$ and then begin to drop. The same qualitative conclusion follows also from Eqn (56) valid for the double exchange.

If this maximal value of Γ approaches 1, then a density range should exist in the vicinity of $n_{\max}$, in which the complete charge-carrier localization in the band tails must occur. This means transition into the insulating state at temperatures sufficiently close to T_C. But outside this range the metal-insulator transition should be absent. Just this situation is realized in the oxygen-poor EuO: the metal-insulator transition occurs at 50 K, i.e. markedly below the Curie point of 67 K for an undoped semiconductor (in a doped sample it should be still higher). The transition is observed at $n \sim (1-2)\times 10^{19}\ \mathrm{cm}^{-3}$, but disappears already at $n \sim 3\times 10^{19}\ \mathrm{cm}^{-3}$ [105].

Not only the temperature-dependent Anderson localization described above but also the Mott localization may lead

to the metal-insulator transition in the degenerate ferromagnetic semiconductors. These mechanisms are essentially different: the former is related to randomness in the impurity distribution, and the latter does only to the Coulomb interaction between electrons (holes) and donors (acceptors). It remains in force at ideally periodic ordering in the positions of the impurity atoms, too.

Qualitatively, the electronic transition from the delocalized states to the localized ones through the Mott mechanism may be explained as follows. The electron delocalization at $T = 0$ is caused by the fact that the electrostatic potential of the donor screened by other delocalized electrons turns out to be insufficiently strong to capture this electron. But at finite temperatures the electron is attracted to the donor by the exchange forces as well, which is described by the effective dielectric constant ζ_0, whose value is reduced as compared with the true dielectric constant ε_0. As was already pointed out, the minimum of ζ_0 is situated at a temperature of the order of T_C. Hence, the effective donor potential is maximal there, and above a certain temperature it may cause the electron localization at an impurity atom.

As a criterion of the temperature Mott metal-insulator transition the following relationship may be proposed, which constitutes natural generalization of the standard Mott criterion:

$$a_B^* n^{1/3} \simeq 0.25, \qquad a_B^* = \frac{\zeta_0}{me^2}\,. \tag{58}$$

A quantitative theory of the metal–insulator transition in degenerate ferromagnetic semiconductors is likely to combine specific features of the Mott and Anderson transitions. It should be noted that appearance of a gap at the Fermi surface at temperatures above the resistivity maximum position (described in Section 5.1) corresponds to the Mott transition mechanism, and not to the Anderson transition mechanism.

If the direct exchange in the semiconductor is antiferromagnetic, then the metal–insulator transition should take place at a density, which is close to the density whereat the magnon frequencies in the ferromagnetic state become nonnegative, but does not coincide with it exactly. This is seen from Eqns (49), (55): at the stability boundary for the ferromagnetic magnon spectrum $\nu_0 = |J|\,S/3t$, the quantity Γ diverges and remains more than 1 over the range from ν_0 to $\nu = \nu_0 + \delta$, where $\delta \propto T^{1/2}$. This signifies the magnetoelectric instability of the system in the region of its magnetic stability ($\Omega_q \geqslant 0$): its effective dielectric constant becomes negative and, according to Eqn (13), the screening of the electrostatic potential disappears. This instability points to the tendency of the system to go over into a nonuniform state [47]. This comprises an additional argument in favour of a nonuniform state of heavily doped samples with a nonsaturated magnetic moment.

If now one goes over to the densities exceeding $\nu_0 + \delta$, then close to this value the system should be formally in the insulating state though the Γ value close to 1 was obtained under assumption of the metallic ferromagnetic state. As was pointed out above, this is a consequence of invalidity of Eqn (57) at such Γ. For this reason it is difficult to make definite conclusions about the singularity in behaviour of the system. At still larger ν the resistivity should display a temperature peak, the height of which should decrease monotonically with increasing ν, in full agreement with experimental data (cf. Fig. 8).

The magnetoresistivity may be analyzed in the same manner. For example, as is seen from Eqns (17), (21), the quantity Γ diminishes with increasing field strength H, and this effect should be maximal in the region where the resistivity peak is located.

6.7 Quantum theory of the canted antiferromagnetic state and its magnetoelectric instability

With the investigators of lanthanum manganites, the idea advanced in Ref. [48] remains very popular that the properties of $La_{1-x}D_xMnO_3$ are determined by the canted antiferromagnetic ordering in them. For this reason it is advisable, in addition to the experimental data contradicting it (Section 3.2), to present theoretical argumentation according to which such a structure should be unstable. In the case of the double exchange the magnon spectrum for the canted antiferromagnetic structure was not found so far, and for this reason investigations of its stability against purely magnetic fluctuations were not carried out yet. But one may prove that it is unstable against the magnetoelectric fluctuations .

De Gennes [48] based his idea on the assumption that the effective hopping integral for an s-electron, modelling a hole in real systems, depends on the angle 2θ between spin moments of two neighbouring atoms in the following manner (compare with Eqn (23)):

$$B = t\cos\theta\,. \tag{59}$$

This expression is a generalization of the expression for the energy of two atoms with classical d-spins of magnitude S, between which an s-electron hops. Condition is used that its hopping integral t is small compared with the (s–d)-energy AS (the double exchange [127]).

But the possibility of such a generalization is not obvious. Certainly, result (59) for a pair of atoms was obtained in Ref. [127] rigorously. But in a crystal consisting of an arbitrary large number of atoms, correlation should exist between electron transitions in various pairs of atoms. An analysis carried out within the framework of a quantum spin model, yields that the accuracy of this expression at $\theta = \pi$ is only of the order of $(2S)^{-1/2}$ and not $1/2S$, as it should be the case for classical spins [47]. This means that at $S = 2$, like is the case for Mn^{4+}, the effective hopping integral at the collinear antiferromagnetic ordering is far from vanishing, remaining comparable to the hopping integral at the ferromagnetic ordering.

This leads to an important physical consequence [47]: the canted antiferromagnetic ordering cannot be more energetically favoured than the collinear antiferromagnetic ordering does at an arbitrarily small charge-carrier density. But even when the charge carrier density is sufficiently large for this condition to be met, all the same, the canted antiferromagnetic ordering turns out to be unstable against the electrostatic fluctuations: they should trigger a nonuniform state of the sample (the phase separation) [47].

A quantum calculation for $A > 0$ [129 – 131] implies rigid fixation of magnetic sublattice spins. In constructing the trial function it is assumed that spins of atoms, from which the s-electrons are absent, are always aligned with the sublattice moments to which they belong. This means that the d-spin deflection from the moment of its sublattice is possible only as a result of its exchange with the s-electron, which is located on it.

Two possibilities are taken into account: (1) the total moment of the s-electron and of the atom, on which it is

located, is parallel to the moment of its sublattice; (2) the projection of their combined spin onto the latter is by 1 less than its maximal value (the corresponding states of the d-spin and of the s-electron located on it are the eigenstates of the (s–d)-exchange Hamiltonian, i.e. of the second term in Eqn (1)).

Taking into account only states of the first type leads to Eqn (59). But accounting also for the states of the second type makes it possible to obtain the following expression for the charge carrier energy:

$$E_{\pm}(\mathbf{k}) = -6B_{\pm}\gamma_{\mathbf{k}}\,, \tag{60}$$

$$B_{\pm} = t(2S+1)^{-1/2}\left[(1+y^2)^{1/2} \pm y\right], \tag{61}$$

$$y = M(2S+1)^{-1/2}\,, \qquad M = S\cos\theta\,,$$

where 2θ is the angle between the sublattice moments, M is the magnetization of the structure.

In the case of the collinear antiferromagnetic ordering both the bands (60), (61) coincide and are of width $(2S+1)^{-1/2}$ times less than the band width in the ferromagnetic state $2zt$, when the total spin of the system is maximal (the 'plus' sign corresponds to it in Eqn (61), whereas the 'minus' sign corresponds to the total spin of the system less by 1). Equation (60) can be obtained from it in the leading order in the standard parameter $1/2S$ for classical spins, if only $M \gg (2S+1)^{1/2}$, i.e. for states close to the ferromagnetic one. The ground-state energy of a system with allowance made for the direct exchange between d-spins is given by the expression

$$E = -3IS^2N\cos 2\theta + \sum\left[E_{+}(\mathbf{k})\,n_{+}(\mathbf{k}) + E_{-}(\mathbf{k})\,n_{-}(\mathbf{k})\right], \tag{62}$$

where $n_{\pm}(\mathbf{k})$ are the Fermi distribution functions for the charge carriers. Given the number of s-electrons per atom v fixed, the angle θ is determined from the condition of the minimal total energy (62).

It follows from Eqns (60) – (62) that in the density range between v_A and v_F the energy of the canted antiferromagnetic ordering is lower than the energies of the collinear ferromagnetic and antiferromagnetic states, where

$$v_A = \left(\frac{\pi}{4}\right)^4\left[2(2S+1)^{3/2}\left|\frac{I}{t}\right|\right]^3, \tag{63}$$

$$v_F = \frac{2}{t}\,|I|\,S(S+1)\,, \tag{64}$$

hence, it cannot be stable certainly at densities v below v_A.

Of subsequent papers on the subject, I would like to mention Ref. [132], where an attempt was also made to develop the quantum theory of the double exchange. But approximations of the mean-field type used there did not allow the results indicated in this section to be reproduced. Recently, the paper [133] was published which is devoted to this subject, too.

Going over to an analysis of the magnetoelectric instability of the canted antiferromagnetic state, it should be emphasized that in this case the quantity Γ is given by Eqn (53) as well. Restricting ourselves to a sufficiently large magnetization, when Eqn (60) is valid, we obtain

$$\Gamma = \frac{9}{2}\,\frac{1}{(6\pi^2)^{2/3}}\,\frac{v^{1/3}}{v_F}\,. \tag{65}$$

As in the degenerate ferromagnetic semiconductors the density v_F is small (this is evident from Eqn (64) with allowance made for the fact that $IS^2 \ll t$), and v is of the same order of magnitude as v_F, the quantity Γ should exceed 1, which, as it was pointed out in the previous section, evidences the instability of the uniform canted antiferromagnetic ordering and the tendency of the system to go over into a nonuniform state.

7. Conclusions

I would like to hope that after reading this review article, the reader will not come to the conclusion that the question is already solved of lanthanum manganites as an undeniable basis for the information technics of future. The outcome of this 'historical' debate between the multilayered magnetic films and lanthanum manganites is not clear yet, and I do not urge the investigators of multilayered systems to finish their studies and go home. I am ready to repeat after the Great Pilot Mao Tse Tung: 'Let a hundred of flowers be in blossom, let a hundred of sciences flourish'.

Certainly, each professional in the basic science is only an amateur in the technical applications. Nevertheless, I venture to express some considerations applied to the applications. Though the properties of magnetic semiconductors as materials with GMR are known for a very long time, people engaged in applications either did not know this, or have forgotten this, or did not want to change the direction of their investigations. In any case, still a few years ago my attempts to remember some of them about magnetic semiconductors were not perceived.

But, instead of this, results of paper [2] were perceived, from which the Renaissance of the magnetic semiconductors began. Though, in principle, in this paper results obtained earlier on lanthanum manganite crystals were only confirmed qualitatively by investigations on their films, obviously, this paper was published at the right time. A wide resonance received by this paper evidences, in particular, that the multilayered systems have problems with applications, which make investigators search for other physical systems with GMR. One cannot tell about the multilayered systems that enough is as good as a feast.

Needless to say, time should elapse between discovery (or rediscovery, as in the case considered) of a physical phenomenon and its practical application. In reality, the time count for the lanthanum manganites began only one year ago, when their massive investigations started. Studies of multilayered systems took incomparably much time. One has already well understood how strongly properties of the lanthanum manganite films depend on technology of their preparation, and some technologies are found which are optimal in comparison with other procedures. As far as I understand technical problems, the main problem for the lanthanum manganite films is the enhancement of their sensitivity to weak magnetic fields.

From the physical point of view, it seems advisable to use for this aim the lanthanum manganite films in the phase-separated ferromagnetic-antiferromagnetic state, when the high-conducting ferromagnetic droplets are separated by insulating antiferromagnetic layers. The probability of the tunnelling between these droplets should sharply increase with the field strength even in weak fields.

Be it as it may, the first practical devices based on the lanthanum manganites are already constructed. I mean a

sensor element — the telephone membrane. The lanthanum manganite film is deposited on the membrane which is placed in a nonuniform magnetic field. The sound vibrations cause displacements of this film in the field and, hence, changes in its resistivity. Respectively, the potential drop across this film also changes. Even without amplifiers the electric response to the sound amounts to a very impressive value of several meV [134].

One may hope that in future much more complicated and effective lanthanum-manganite-based devices than such simple sensors will be constructed.

References

1. Fullerton E *Appl. Phys. Lett.* **63** 1699 (1993)
2. Jin S et al. *Science* **264** 413 (1994)
3. Shapira Y et al. *Phys. Rev. B* **10** 4765 (1974)
4. Gong G et al., in *40th Annual Conference Magnetism and Magnetic Materials. Abstracts* (Philadelphia, Pennsylvania, 1995) p. 20
5. Hwang H et al., in *40th Annual Conference Magnetism and Magnetic Materials. Abstracts* (Philadelphia, Pennsylvania, 1995) p. 21
6. Zhang S, in *40th Annual Conference Magnetism and Magnetic Materials. Abstracts* (Philadelphia, Pennsylvania, 1995) p. 21
7. Ogale C et al., in *40th Annual Conference Magnetism and Magnetic Materials. Abstracts* (Philadelphia, Pennsylvania, 1995) p. 22
8. Canedy C, Ibsen K, Gang Xiao, in *40th Annual Conference Magnetism and Magnetic Materials. Abstracts* (Philadelphia, Pennsylvania, 1995) p. 22
9. McGuire T et al., in *40th Annual Conference Magnetism and Magnetic Materials. Abstracts* (Philadelphia, Pennsylvania, 1995) p.22
10. Lu H et al., in *40th Annual Conference Magnetism and Magnetic Materials. Abstracts* (Philadelphia, Pennsylvania, 1995) p.23
11. Sharma R et al., in *40th Annual Conference Magnetism and Magnetic Materials. Abstracts* (Philadelphia, Pennsylvania, 1995) p. 23
12. Byers J, in *40th Annual Conference Magnetism and Magnetic Materials. Abstracts* (Philadelphia, Pennsylvania, 1995) p. 24
13. Vas'ko V et al., in *40th Annual Conference Magnetism and Magnetic Materials. Abstracts* (Philadelphia, Pennsylvania, 1995) p. 24
14. Anane A et al., in *40th Annual Conference Magnetism and Magnetic Materials. Abstracts* (Philadelphia, Pennsylvania, 1995) p. 25 (*J. Phys.* (*Sol. St.*) **7** 7015 (1995))
15. Satpathy S et al., in *40th Annual Conference Magnetism and Magnetic Materials. Abstracts* (Philadelphia, Pennsylvania, 1995) p. 25 (*Phys. Rev. Lett.* **76** 960 (1996))
16. Park J-H et al., in *40th Annual Conference Magnetism and Magnetic Materials. Abstracts* (Philadelphia, Pennsylvania, 1995) p. 25
17. Zhang W, Boyd I, in *40th Annual Conference Magnetism and Magnetic Materials. Abstracts* (Philadelphia, Pennsylvania, 1995) p. 26
18. Zou Liang-Jian et al., in *40th Annual Conference Magnetism and Magnetic Materials. Abstracts* (Philadelphia, Pennsylvania, 1995) p. 163
19. Xiong G et al., in *40th Annual Conference Magnetism and Magnetic Materials. Abstracts* (Philadelphia, Pennsylvania, 1995) p. 163
20. Lofland S et al., in *40th Annual Conference Magnetism and Magnetic Materials. Abstracts* (Philadelphia, Pennsylvania, 1995) p. 164 (*Phys. Rev. B* **52** 15058 (1995))
21. Krishnan K, Modak A, Lucas G, in *40th Annual Conference Magnetism and Magnetic Materials. Abstracts* (Philadelphia, Pennsylvania, 1995) p. 164
22. Dionne G, in *40th Annual Conference Magnetism and Magnetic Materials. Abstracts* (Philadelphia, Pennsylvania, 1995) p. 165
23. Ibarra M et al., in *40th Annual Conference Magnetism and Magnetic Materials. Abstracts* (Philadelphia, Pennsylvania, 1995) p. 165
24. Arnold Z et al., in *40th Annual Conference Magnetism and Magnetic Materials. Abstracts* (Philadelphia, Pennsylvania, 1995) p. 166
25. Nunez-Regueiro J et al., in *40th Annual Conference Magnetism and Magnetic Materials. Abstracts* (Philadelphia, Pennsylvania, 1995) p. 166
26. Fontcuberta J et al., in *40th Annual Conference Magnetism and Magnetic Materials. Abstracts* (Philadelphia, Pennsylvania, 1995) p. 167 (*Phys. Rev. Lett.* **76** 1122 (1996))
27. Srinivasan G, in *40th Annual Conference Magnetism and Magnetic Materials. Abstracts* (Philadelphia, Pennsylvania, 1995) p. 167
28. Li Z, Zeng X, Wong H, in *40th Annual Conference Magnetism and Magnetic Materials. Abstracts* (Philadelphia, Pennsylvania, 1995) p. 168
29. Tokura Y, in *40th Annual Conference Magnetism and Magnetic Materials. Abstracts* (Philadelphia, Pennsylvania, 1995) p. 196
30. Ramesh R et al., in *40th Annual Conference Magnetism and Magnetic Materials. Abstracts* (Philadelphia, Pennsylvania, 1995) p. 196
31. Hundle M et al., in *40th Annual Conference Magnetism and Magnetic Materials. Abstracts* (Philadelphia, Pennsylvania, 1995) p. 20
32. Takeda T L, Ohara S *J. Phys. Soc. Jpn.* **37** 275 (1974)
33. Yakel H L *Acta Crystallogr.* **8** Pt7 394 (1955)
34. Wollan E O, Koehler W C *Phys. Rev.* **100** 545 (1955)
35. Fesenko E G *Semeĭstvo Perovskita i Segnetoélektrichestvo* (Perovskite Family and Segnetoelectricity) (Moscow: Atomizdat, 1972)
36. Emsley J *Elements* (Oxford: Clarendon Press, 1991)
37. Kugel' K I, Khomskiĭ D I *Usp. Fiz. Nauk* **136** 621 (1982) [*Sov. Phys. Usp.* **24** 231 (1982)]
38. Troyanchuk I O *Zh. Eksp. Teor. Fiz.* **102** 251 (1992) [*Sov. Phys. JETP* **75** 251 (1992)]
39. Matsumoto G *IBM J. Res. Develop.* **14** 258 (1970)
40. Matsumoto G *J. Phys. Soc. Jpn.* **29** 606, 615 (1970)
41. Elemans J *J. Solid State Chem.* **3** 238 (1971)
42. Urushibara A at al. *Phys. Rev. B* **51** 14103 (1995)
43. Pickett W, Singh D *Europhys. Lett.* **32** 759 (1995)
44. Sarma D et al. *Phys. Rev. Lett.* **75** 1126 (1995)
45. Jonker G H, van Santen J H *Physica* **16** 337 (1950)
46. Izyumov Yu A, Ozerov R P *Magnitnaya Neitronografiya* (Magnetic Neutronography) (Moscow: Nauka, 1966)
47. Nagaev E L *Fizika Magnitnykh Poluprovodnikov* (Physics of Magnetic Semiconductors) (Moscow: Nauka, 1979) [Translated into English (Moscow: Mir, 1983)]
48. De Gennes P–G *Phys. Rev.* **118** 141 (1960)
49. van Santen J H, Jonker G H *Physica* **16** 559 (1950)
50. Nagaev E L *Zh. Eksp. Teor. Fiz.* **54** 228 (1968) [*Sov. Phys. JETP* **27** 112 (1968)]
51. Gubkin M K et al. *Pis'ma Zh. Eksp. Teor. Fiz.* **60** 56 (1994) [*JETP Lett.* **60** 57 (1994)]
52. Perekalina T M et al. *Fiz. Tverd. Tela* **32** 3146 (1990)
53. Jia Y et al. *Phys. Rev. B* **52** 9147 (1995)
54. Troyanchuk I O, Pastushonok S N *Fiz. Tverd. Tela* **31** 302 (1989) [*Sov. Phys. Solid State* (USA) **31** 1830 (1989)]
55. Krinchik G S, Gan'shina E A, Trifonov A Yu *Fiz. Tverd. Tela* **33** 1607 (1991)
56. Gupta A et al. *Appl. Phys. Lett.* **67** 3494 (1995)
57. Morimoto Y, Asamitsu A, Tokura Y *Phys. Rev. B* **51** 16491 (1995); Tamura S *J. Magn. Magn. Mater.* **31–34** 805 (1983)
58. Schiffer P et al. *Phys. Rev. Lett.* **75** 3336 (1995)
59. Radaelly P et al. *Phys. Rev. Lett.* **75** 4488 (1995)
60. Asamitsu A et al. *Nature* (New York) **373** 407 (1995)
61. Ibarra M et al. *Phys. Rev. Lett.* **75** 3541 (1995)
62. Perekalina T M et al. *Fiz. Tverd. Tela* **32** 1242 (1990)
63. Nagaev E L *Zh. Eksp. Teor. Fiz.* **56** 1013 (1969) [*Sov. Phys. JETP* **29** 545 (1969)]; *Fiz. Metallov Metalloved.* **29** 905 (1970); *Phys. Status Solidi* (b) **65** 11 (1974)
64. Nagaev E L *Pis'ma Zh. Eksp. Teor. Fiz.* **16** 558 (1972) [*JETP Lett.* **16** 394 (1972)]; Kashin V A, Nagaev E L *Zh. Eksp. Teor. Fiz.* **66** 2105 (1974) [*Sov. Phys. JETP* **39** 1036 (1974)]
65. Nagaev E L *Phys. Status Solidi* (b) **186** 9 (1994)
66. Nagaev E L *Usp. Fiz. Nauk* **165** 529 (1995) [*Phys. Usp.* **38** 497 (1995)]
67. Nagaev E L *Physica C* **222** 324 (1994)
68. Nagaev E L *Z. Phys. B* **98** 59 (1995)
69. Nagaev E L *Physica C* **265** 267 (1996)
70. Oliveira N F (Jr) et al. *Phys. Rev. B* **5** 2634 (1972)
71. Saitoh T et al. *Phys. Rev. B* **51** 13942 (1995)
72. (a) Nagaev E L *Phys. Lett. A* **218** 367 (1996); (b) Tamura S *Phys. Lett. A* **78** 401 (1980)

73. Knizek K et al. *J. Sol. St. Chem.* **100** 292 (1992)
74. Tomioka Y et al. *Phys. Rev Lett.* **74** 5108 (1995)
75. Pollert E, Krupicka S, Kuzmicova E *J. Phys. Chem. Solids* **43** 1137 (1982)
76. Jirak Z et al. *J. Mag. Mag. Mater.* **15–18** 519 (1980)
77. Jirak Z et al. *J. Mag. Mag. Mater.* **53** 153 (1985)
78. Yoshizawa H et al. *Phys. Rev. B* **52** R13145 (1995)
79. Tomioka Y et al. *Phys. Rev. B* **53** R1689 (1996)
80. Lees M et al. *Phys. Rev. B* **52** 14303 (1995)
81. Yu I, Senna M *Appl. Phys. Lett.* **66** 424 (1995)
82. Kuwahara H et al. *Science* **270** 961 (1995)
83. Chen C, Cheong S-W, Cooper A *Phys. Rev. Lett.* **71** 2461 1993); Cheong S-W et al. *Phys. Rev. B* **49** 7088 (1994); Battle P, Gibb T, Lightfoot P *J. Solid State Chem.* **84** 271 (1990)
84. Tokura Y et al *J. Phys. Soc. Jpn.* **63** 3931 (1994)
85. Belov K P, Svirina E P, Portugal O E *Fiz. Tverd. Tela* **20** 3492 (1978) [*Sov. Phys. Solid State* **20** 2021 (1978)]
86. Svirina E P et al. *Fiz. Tverd. Tela* **20** 309 (1978) [*Sov. Phys. Solid State* **20** 180 (1978)]
87. Perekalina T M et al. *Fiz. Tverd. Tela* **31** (9) 87 (1989)
88. Haupt L et al. *Solid State Commun.* **72** 1093 (1989)
89. Okimoto Y et al. *Phys. Rev. Lett.* **75** 109 (1995)
90. (a) Chainani A, Mathew H, Sarma D *Phys. Rev. B* **47** 15397 (1993); (b) Asamitsu A, Morimoto Y, Tokura Y *Phys. Rev. B* **53** R2952 (1996)
91. Searle C W, Wang S T *Can. J Phys.* **47** 2703 (1969)
92. Gubkin M K et al. *Fiz. Tverd. Tela* **35** 1443 (1993); Perekalina T M et al. *Fiz. Tverd. Tela* **33** 681 (1991)
93. Belov K P, Svirina E P, Shlyakhina L P *Fiz. Tverd. Tela* **26** 1903 (1984) [*Sov. Phys. Solid State* **26** 1156 (1984)]
94. Kusters R M et al. *Physica B* **155** 362 (1989)
95. Itoh M et al. *Phys. Rev. B* **52** 12522 (1995)
96. Khazeni K et al. *Phys. Rev. Lett.* **76** 295 (1996)
97. Mahendiran R, Mahesh R, Raychaudhuri A *Solid State Commun.* **94** 513 (1995)
98. Von Helmolt R, Wecker J, Holzapfel B *Phys. Rev. Lett.* **71** 2331 (1993)
99. Ju H, Lo H *Appl. Phys. Lett.* **65** 2108 (1994)
100. Tanaka J et al. *J. Phys. Soc. Jpn.* **51** 1236 (1982)
101. Manoharan S et al. *J. Appl. Phys.* **76** 3923 (1994)
102. Chahara K et al. *Appl. Phys. Lett.* **63** 1990 (1993)
103. Huang H et al. *Phys. Rev. B* **52** 914 (1995)
104. Xiong G et al. *Appl. Phys. Lett.* **66** 1427 (1995); **67** 3031 (1995)
105. Oliver M R et al. *Phys. Rev Lett.* **24** 1064 (1970); Penny T, Shafer M, Torrance J *Phys. Rev. B.* **5** 3669 (1972); Shapira Y, Foner S, Reed T *Phys. Rev. B* **8** 2299 (1973)
106. Yanase A, Kasuya T *J. Phys. Soc. Jpn.* **25** 1025 (1968); Umehara M, Kasuya T *J. Phys. Soc. Jpn.* **40** 13 (1976)
107. Nagaev E L *Zh. Eksp. Teor. Fiz.* **90** 652 (1986) [*Sov. Phys. JETP* **63** 379 (1986)]; *Zh. Eksp. Teor. Fiz.* **92** 569 (1987) [*Sov. Phys. JETP* **65** 322 (1987)]; *Fiz. Tverd. Tela* **29** 385 (1987) [*Sov. Phys. Solid State* **29** 220 (1987)]; *Phys. Lett. A* **211** 313 (1996); *Phys. Lett. A* **215** 321 (1996); *Phys. Rev. B* (in press)
108. Coey J et al. *Phys. Rev. Lett.* **75** 3910 (1995)
109. Furakawa N *J. Phys. Soc. Jpn* **64** 3164 (1995)
110. Fa-jian Shi, Meng Ding, Tsung-han Lin *Solid State Commun.* **96** 931 (1995)
111. Millis A J, Littlewood P B, Shraiman B I *Phys. Rev. Lett.* **74** 5144 (1995)
112. Inoue J, Maekawa S *Phys. Rev. Lett.* **74** 3407 (1995)
113. Kim D J, Schwartz B B, Praddaude H H *Phys. Rev. B* **7** 205 (1972)
114. Kim D J, Schwartz B B *Phys. Rev. Lett.* **28** 310 (1972); *Phys. Rev. B* **15** 377 (1977); Gunnarson O, Lundqvist B, Lundqvist S *Solid State Commun.* **11** 149 (1972)
115. Grigin A P, Nagaev E L *Fiz. Tverd. Tela* **17** 2614 (1975)
116. Nagaev E L, Grigin A P *Pis'ma Zh. Eksp. Teor. Fiz.* **20** 650 (1974) [*JETP Lett.* **20** 299 (1974)]
117. Nagaev E L *Zh. Eksp. Teor. Fiz.* **56** 1013 (1969) [*Sov. Phys. JETP* **29** 545 (1969)]
118. Nagaev E L *Fiz. Tverd. Tela* **11** 2779 (1969)
119. (a) Nagaev E L, Grigin A P *Phys. Status Solidi* (b) **65** 457 (1974); (b) Nagaev E L *Phys. Lett. A* **219** 101 (1996)
120. Elliott R J, Wedgwood F A *Proc. Phys. Soc.* **81** 846 (1963)
121. Elliott R J, Wedgwood F A *Proc. Phys. Soc.* **84** 63 (1964)
122. Nagaev E L, Zil'bervarg V E *Fiz. Tverd. Tela* **17** 1261 (1975)
123. Nagaev E L, Zil'bervarg V E *Solid State Commun.* **16** 823 (1975)
124. Nagaev E L *Solid State Commun.* **15** 109 (1974)
125. Landau L D, Lifshits E M *Statisticheskaya Fizika.* Chast' 1 (Statistical Physics Part 1) p. 1 (Moscow: Nauka, 1976) [Translated into English (Oxford, New York: Pergamon Press, 1980)]
126. Zener C *Phys. Rev.* **82** 403 (1951)
127. Anderson P W, Hasegawa H *Phys. Rev.* **100** 675 (1955)
128. Zil'bervarg V E, Nagaev E L *Fiz. Tverd. Tela* **16** 2834 (1974) [*Sov. Phys. Solid State* **16** 1838 (1974)]
129. Nagaev E L *Fiz. Tverd. Tela* **13** 1321 (1971)
130. Nagaev E L *Fiz. Tverd. Tela* **14** 773 (1972) [*Sov. Phys. Solid State* **14** 658 (1972)]
131. Nagaev E L *Zh. Eksp. Teor. Fiz.* **57** 1274 (1969)[*Sov. Phys. JETP* **30** 693 (1970)]
132. Kubo K, Ohata N *J. Phys. Soc. Jpn.* **33** 21 (1972)
133. Okube T *J. Phys. Soc. Jpn.* **64** 3442 (1995)
134. Jin S et al. *J. Appl. Phys.* **76** (10) 1552 (1994)